Universität Heidelberg
Interdisciplinary Center for Scientific Computing
Engineering Mathematics and Computing Lab

Bachelor Thesis

Continuous Modeling of Extracellular Matrix Invasion by Tumor Growth

Name: Maximilian Bing
Matriculation number: 3606060
Advisor: Professor Vincent Heuveline
Date of submission: April 20, 2024

Hiermit versichere ich, dass ich die Arbeit selbst verfasst und keine anderen als die angegebenen Quellen und Hilfsmittel benutzt und wörtlich oder inhaltlich aus fremden Werken Übernommenes als fremd kenntlich gemacht habe. Ferner versichere ich, dass die übermittelte elektronische Version in Inhalt und Wortlaut mit der gedruckten Version meiner Arbeit vollständig übereinstimmt. Ich bin einverstanden, dass diese elektronische Fassung universitätsintern anhand einer Plagiatssoftware auf Plagiate überprüft wird.

_____

Abgabedatum:

Zusammenfassung

Krebszellen können sich vom Primärtumor lösen und das umgebende Gewebe abbauen. Kontinuierliche mathematische Modelle wurden in der Vergangenheit mehrmals verwendet, um diesen Prozess besser zu verstehen.
In diesem Zusammenhang basieren die Modelle in der Regel auf mindestens drei Schlüsselkomponenten: den Tumorzellen, dem umgebenden Gewebe oder der extrazellulären Matrix (ECM) und den matrixabbauenden Enzymen (MDE). Diese Variablen werden in dem hier behandelten Modell in einem System partieller Differentialgleichungen gekoppelt um den komplexe Prozess der Tumor Invasion zu beschreiben.
Da ein solches Modell ein hohes Mas an Freiheitsgraden besitzt, hat eine Konfiguration der Parameter des Modells hohen Einfluss auf die produzierten Ergebnisse.
Diese Arbeit untersucht den Einfluss der Wahl dieser Konfigurationen sowie auch den der Dimension auf die Ergebnisse einer Simulation.
In der Literatur werden fast ausschlieslich eindimensionalen Experimente beschrieben, daher werden die Experimente hier nur in hoeheren Dimensionen durchgeführt, zwei oder drei dimensional. Darüber hinaus wurde hauptsächlich die homogene Struktur der extrazellulären Matrix (ECM) behandelt, jedoch fuer eine heterogene extrazelluläre Matrix Struktur nur solche Faelle analysiert, die wenig biologische Relevanz haben. Die Struktur der epithelialen Schicht und der benachbarten extrazellulären Matrix ist jedoch in biologischem Gewebe organisierter als in den meisten später gezeigten Simulationen und anderen Beispielen aus der Literatur. Diese Organisiertheit kann zu erheblichen Veränderungen der Ergebnisse führen, selbst wenn die Parameter konstant gehalten werden.
Um realitätsnahe biologische Szenarien zu simulieren, verlangen Simulationen mindestens zwei räumlichen Dimensionen. Daher soll diese Arbeit einen Einstiegspunkt geben um das zu grundliegende Modell fuer solche Simulationen zu nutzen. Die Parameteranalyse soll hierbei auch helfen eine angebrachte Wahl der Parameter zu erleichtern.

Abstract

Cancer cells have the ability to detach from the primary tumor and degrade the surrounding tissue. Continuous mathematical models have been utilized in the past to better understand this process.
In this context, these models typically rely on at least three key components: tumor cells, the surrounding tissue or extracellular matrix (ECM), and matrix-degrading enzymes (MDE). These variables are coupled in a system of partial differential equations to describe the complex process of tumor invasion.
Due to the high degree of freedom of such a model, the configuration of the model parameters significantly influences the resulting outcomes. This study investigates the impact of choosing these configurations, as well as the dimensionality, on the results of a simulation.
In the literature, predominantly one-dimensional experiments are described, hence the experiments conducted here are performed in higher dimensions, two or three dimensional. Furthermore, while the homogeneous structure of the extracellular matrix (ECM) has been mainly addressed, cases involving a heterogeneous extracellular matrix structure have been analyzed to a lesser extent, despite their limited biological relevance.
However, the structure of the epithelial layer and the adjacent extracellular matrix in biological tissue is more organized than in most simulations and other examples presented in the literature. This organization can lead to significant changes in results, even when parameters are held constant.
To simulate realistic biological scenarios, simulations require at least two spatial dimensions. Therefore, this work aims to provide a starting point for utilizing the underlying model for such simulations. The parameter analysis aims to facilitate an appropriate selection of parameters.

Contents

1 Introduction

Modelling tumor growth plays a key role in understanding the complex mechanisms, governing development and progression of cancer diseases. Since cancer is one of the leading death causes worldwide and many of its forms are incurable, challenges in the area of Oncology require researchers to have a deep understanding in as well the biological foundation, which lead to malignant cell mutation and factors for tumor growing and spreading, as well as the mathematical models used for simulating these events. This Bachelorthesis is dedicated to analyse Anderson et al.'s [1, 2] model for tumor modelling. The dynamics of tumerous growth are an intricate system, which is influenced by numerous biological and chemical factors, as well as genetic pre-dispostitions, the surrouding tissue of cancer cells, angiogene processes and interactions with the immune system. The integration of these factors in mathematical models allow us to decode these complex interactions with quantification and help us understand the fundamental mechanisms, which surroud cancerous diseases.
Mathematical models are a very important part in Oncology, they are used to quantify biological phenomena and therefore help to predict and understand tumor development and treatment response. In Mathematical Oncology we differentiate between continuous, discrete and hybrid models [3]. For the continuous type, cells and tissue are described over time with partial differential equations modelling continuous quantities like in our case the tumour cell density or extracellular matrix concentration.
In the discreate case, an entity-based model is used, pursued with the goal to better understand the phenoma on cell level. This approach allows the researcher to better implement biological effects a cell has with its outer circumstances, like interaction with other cells, nutrients or other microorganisms. As the name implies use these models discrete values to describe the temporal course of events.
Hybrid models try to combine both approaches, to offer efficient systems capturing cell level events as well as continuous changes in outer circumstances.
This work investigates how a continuous model proposed by Anderson et al. [1, 2], to analyse tumour development in the early stages of a cancer disease, performs in the case of different dimensions and free parameter values. The model examines the first two stages of a cancer disease; tumor initiaition, where the tumor cells are localized to a small area and have not yet spread throughout the body; and tumor promotion, with the tumor cells growing and proliferating, invading the surrounding tissue [4]. From examples of the original paper we can already see that the model's results vary with the dimensionality of the space we are modelling the partial differential equations in. Our main focus lies on comparing simulations of two dimensions with those of three dimensions of extracellular matrix invasion by the tumor growth. Additionally to the variation of dimensions we will have a brief look on how the geometry of the extracellular matrix will influence the tumor development.
Another point of interest is the investigation of how the model's free parameters influence the tumor dynamics growth. An important task is to give those parameters a biological meaning and to eventually gain insight into how to adjust them to make the simulation more realistic.

2 Theoretical Basics

2.1 Basics of Tumor Biology

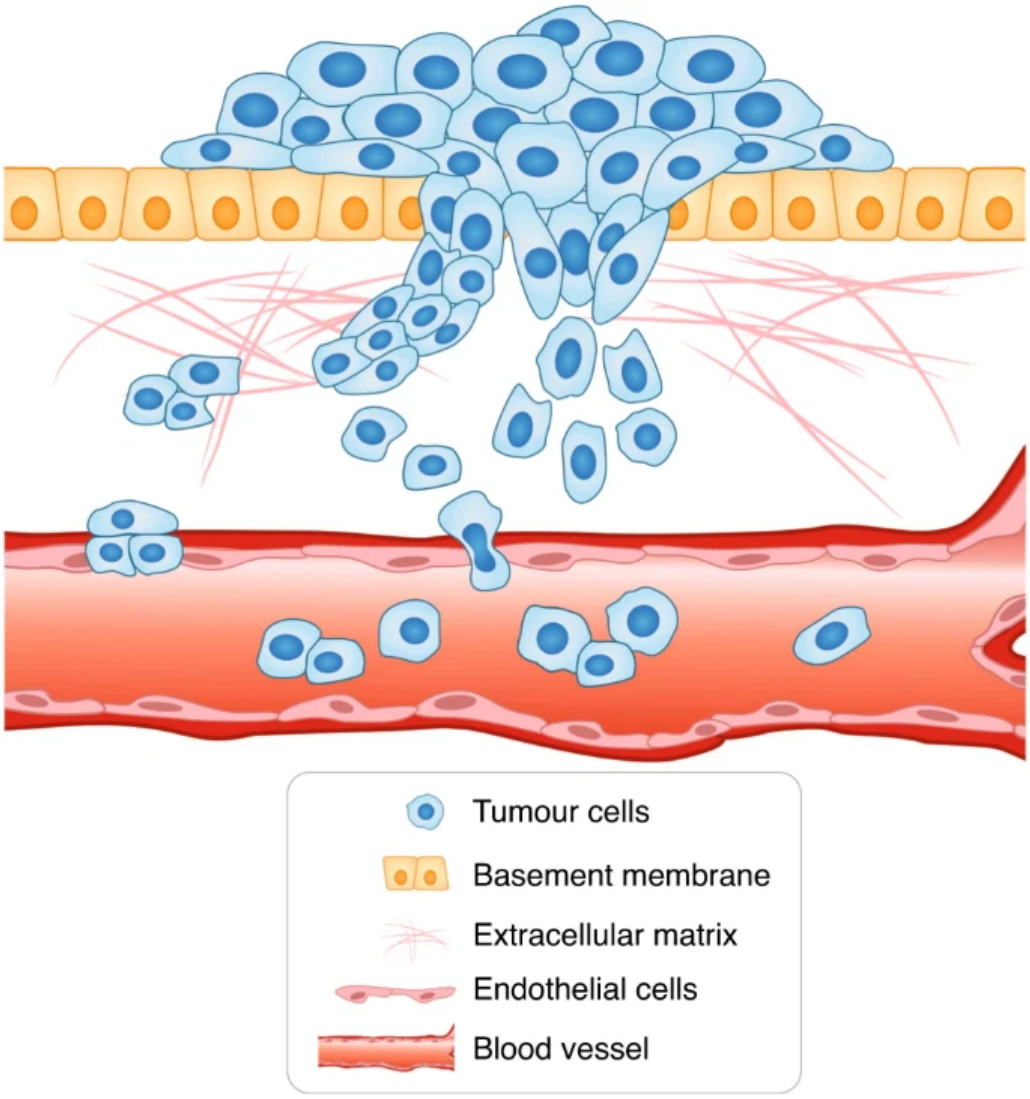

FIGURE 1. Tumor Invasion Stage

The body of a living creature is made up of more than 200 different types of cells, the coordination between the cells and their surroundings keep the body running. Each of these cells is built from the genetic information encoded in the DNA, located in the cells' nuclei. Though the nucleotide sequence of DNA is well checked and maintained throughout the cell's life, mutations still occur that cause the changes in the DNA of a cell. These mutations may be of a positive, negative or neutral nature. In the case of a negative mutation this alternation of the DNA may cause diseases, with cancer being one of them. The failure of the complex system managing cell birth, proliferation, and cell death (apoptosis) causes cancer, resulting in an uncontrolled cell proliferation in a at first

local area. A conglomeration of cancer cells is called a tumor.
Cancer diseases typically follows five stages. First the tumor initiation phase where it comes to the above explained genetic mutations of normal cells. The next stage is the tumor promotion stage, in which the mutated cells of phase one may experience further genetic alterations, with the result of uncontrolled growth and proliferation of the cancerous cells. The third stage is the tumor progression stage, where the cancerous cells progress in growing and proliferating, reaching a critical mass, they form a tumor at a local site of the body. Fourth comes the invasion stage, which is shown in figure 1. Here the tumor is able to invade surrouding tissue by breaking through the cellular membrane, invading the extracellular matrix inside and entering the blood circulation system or the lymphatic system. Next the tumor cells which have invaded the blood circulation of lymphatic system spread throughout the body and form new tumors. This stage is called Metastization. To further grow the tumors need to have access to nutrient and oxygen supply. During angiogensis a tumor develops blood vessels of its own securing its nutritional provision. At this stage first symptoms of host may appear, enabling medical treatment.
In our model the focus lies on the first two stages; tumor invasion and tumor progression. The tumor invasion stage is characterized by the malignant cells gaining the ability to penetrate and invade the surrouding tissue. The tumor cells break through the normal tissue barrier and infiltrate neighboring structures. In order to do so the cancer cells produce so called matrix-degrading enzymes which break down the extracellular matrix. This not only helps local spreading, but also destroys otherwise healthy tissue and cells in the affected area. In the next phase the tumor progression stage, the tumor has grown larger and the cancerous cells take on more aggressive behaviour, by invading the surrounding area further. Whilst they keep growing uncontrolled they are also affected by further genetic instabilities, which lead to more mutations, resulting possibly in the development of resistence mechanisms against for example degrading factors. Already in this stage the affected area is exposed to heavy tissue damage and functional disabilities.
The most important factors influencing those two phases are the genetic dispositions of the tumor cells towards proliferation and the evasion of apoptosis, programmed cell death, which increase the invasive potential. Another important factor is the geometry of the extracellular matrix, as well as the exact macromolcules which make it up. A strong immune biological defense reaction also helps the body defend against the spreading of the cancer cells, so evasion of detection and destruction of the tumor cells plays a key role for the first stages. To invade the affected area the malignant cells need to be able to move freely and fastly. In order to do so cancer cells can gain the ability to lose adhesion properties which healthy cells normally have, to allow migrating into surrouding tissue.

2.2 Mathematical Methods in Oncology

Mathematical methods and models in Oncology play a crucial role in analysing, understanding and predicting cancer development. Since the obejctive of this research underlies complex and intricate biochemical systems and mechanisms, there exist many models, which find their respective application in distinct areas of this research field. These meth-

ods can be coarsely divided into three sections; continuous, discrete and hybrid models [3]. For describing tumor growth, exponential and logisitc growth models are often used, the later allowing limiting factors to play a role during modelling. These methods are a subclass of the differential equations approach which base their functionality on an ordinary or partial differential equation, studying the continuous approach. Like in our model they are not limited to consist of only one equation but can of many, incorporating systematic dependencies on other factors. These models in general deal with continuous quantities like densities, or concentrations, for example spacial and temporal nutritional supply or drug concentration, as well as their effects on the affected area over time. Discrete models use discrete entities to describe the behaviour of tumour cells and their interactions with surrouding tissue. They allow to model a wide range of biological and chemical processes which are hard to describe continuously. Common used types in mathematical oncology are for example Cellular Automata or Agent-Based Models. Cellular Automata represent cells as entities with states on a grid, with each cell being allowed to change states according to a set of rules based on its own current state and the states of the neighbors, whereas Agent-Based Models enable a differentiation of types of cells and allow movement that is not restricted to a grid implementing complex mechanics on cell-cell or cell-environment levels. Using these discrete models allows researchers to focus on biological effects during modelling, which are hard to describe in continuous models. With these approaches we can also simulate genetic and evolutionary events. For example studying the genetic alternations of tumor cells or the interaction between healthy and cancerous cells.
Hybrid models combine both aforementioned methods, of using both continuous and discrete approachese. Like in the model proposed by Franssen et al. [5] or Anderson et al. [1], these approaches allow to incorporate the exactness of continuous models with a wide range of biological effects described by discrete models.
But not all models try to model tumor growth, there are others concerning for example optimality regarding drug dosages or radiation exposition, offering personalized treatment, or Machine Learining and Data Mining methods analysing large datasets, to identify patters and predict outcomes. The later method may be used in all kinds of applications, for example spacial or temporal cancer development but also for drug dosage optimization for individual patients. Putting all these methods together gives us an powerful toolbox to simulate and understand cancer biology. Like the last years have shown they are applied in a wide range, offering insight for all areas of cancer research. Therefore it is important not only to come up with methods but to also evaluate their usefulness and meaningfulness regarding different areas of research.

3 Modelling

3.1 Mathematical Formulation

The model propsed by Anderson et al. [1, 2] and Chaplain et al. [1, 5, 6], extended with terms for modelling cell proliferation and extracellular matrix renewal consists of a system of coupled partial differential equations with zero-flux boundry conditions:

$$\frac{\partial c}{\partial t} = D_c \Delta c - \chi \nabla \cdot (c \nabla e) + \mu_1 c \left(1 - \frac{c}{c_0} - \frac{e}{e_0}\right) \tag{1}$$

$$\frac{\partial e}{\partial t} = -\delta m e + \mu_2 c \left(1 - \frac{c}{c_0} - \frac{e}{e_0}\right) \tag{2}$$

$$\frac{\partial m}{\partial t} = D_m \Delta c + \mu_3 c - \lambda m \tag{3}$$

$$\zeta \cdot (-D_c \nabla c + c \chi \nabla e) = 0 \tag{4}$$

$$\zeta \cdot (-D_m \nabla m) = 0 \tag{5}$$

with the free parameters D_c, D_m, χ, δ, μ_1, μ_2, μ_3 and λ.
The variable c describes the tumor cell density, e the concentration of the extracellular matrix and m the matrix-degrading enzyme concentration. All of those functions are mathematically defined to be mapping a 1,2 or 3 dimensional spacial value x and a temporal value t to a scalar value describing the respective quantity at a specific point in space and time (x, t), $\{c, e, m\} : \mathbb{R}^3 \times \mathbb{R} \to \mathbb{R}$.
To derive the expression of the tumor cell density c we are going to assume that the tumor cell's movement is subject to two influences, haptotaxis and random movement. Haptotaxis is a directed migratory response of cells to gradients of fixed or bound chemicals [1] and random movement is influenced by for example mechanical stress, electric charge or other such physical effects [7]. To get an expression for how much or how fast the tumor cells move, we need to define what flux is. Flux is defined to be the amount of a substance which crosses a unit area in unit time. Incorporating the two assumed influencing factors into our mathematical model we define the haptotatic flux J_{hapto} and random flux J_{random}:

$$J_{hapto} = \chi c \nabla e$$
$$J_{random} = -D_c \nabla c$$

χ is the haptotactic flux coefficient and D_c is a random mobility coefficient. In general these Parameters could also be a function of both extracellular matrix and matrix-degrading enzyme concentration. Knowing that cells grow over time and proliferate, we want to respect this in our model with a term for tumor cell proliferation: $\mu_1 c(1 - \frac{c}{c_0} - \frac{e}{e_0})$. The idea is that this term describes the cell proliferation with a logisitic growth model respecting spacial limiting factors of already present extracellular matrix molecules and tumour cells, μ_1 describes the rate at which proliferation happens. In the initial model proposed by Anderson et al. [1, 2] and Chaplain et al. [1, 5, 6, 8], they did not respect

proliferation of tumor cells and extracellular matrix renewal and applied a conservation equation for the tumor cells which yields:

$$\frac{\partial c}{\partial t} = -\nabla \cdot (J_{hapto} + J_{random})$$
$$\frac{\partial c}{\partial t} = -\nabla \cdot (\chi c \nabla e - D_c \nabla c)$$
$$\frac{\partial c}{\partial t} = D_c \Delta c - \chi \nabla \cdot (c \nabla e)$$

The extended model incorporates proliferation and renewal into this conservation formula resulting in equation 1:

$$\frac{\partial c}{\partial t} = -\nabla \cdot (J_{hapto} + J_{random}) + \mu_1 c(1 - \frac{c}{c_0} - \frac{e}{e_0})$$
$$\frac{\partial c}{\partial t} = D_c \Delta c - \chi \nabla \cdot (c \nabla e) + \mu_1 c(1 - \frac{c}{c_0} - \frac{e}{e_0})$$

To model the extracellular-matrix concentration e, we assume that the enzymes degrade the extracellular matrix upon contact. This assumption is simply modeled by the equation:

$$\frac{\partial e}{\partial t} = -\delta m e$$

where δ is a positive constant describing this degradation process. For the extended model we add a term describing the renewal process of the extracellular matrix:

$$\frac{\partial e}{\partial t} = -\delta m e + \mu_2 c(1 - \frac{c}{c_0} - \frac{e}{e_0})$$

with mu_2 being the coefficient describing the rate of the renewal process.
Modelling the matrix-degrading enzyme concentration m, we combine a diffusion term with production and decay terms. The diffusion term is described like in tumor cell concentration, with the addition that haptotatic fluxes are neglected and only random mobility is assumed, $J_{random} = -D_m \nabla m$. The production term depends on the tumor cell density c and the decay term on the extracellular matrix concentration m. Incorporating this gives us equation 3:

$$\frac{\partial m}{\partial t} = \nabla \cdot J_{random} + \mu c - \lambda e$$
$$\frac{\partial m}{\partial t} = D_m \Delta m + \mu_3 c - \lambda m$$

μ_3 and δ describing production and decay coefficients .

3.2 Numerical Formulation and Parameters

To make solving the model easier we are first going to non-dimensionalise all the equations 1 to 5 in a standard way, with the goal to rescale the space domain to a unit size

domain Ω. For one space dimension this results in the unit interval $[0,1]$, for two the unit square $[0,1]\times[0,1]$ and for three spacial dimensions the unit cube $[0,1]\times[0,1]\times[0,1]$. We start with non-dimensionalising the three continuous variables c, e, m:

$$\tilde{c} = \frac{c}{c_0}$$
$$\tilde{e} = \frac{e}{e_0}$$
$$\tilde{m} = \frac{m}{m_0}$$

Next we rescale distance with an appropriate length scale L (e.g. the maximum invasion distance of the cancer at this early stage of invasion $0.1-1cm$) and time with $\tau = \frac{L^2}{D}$ (D being a chemical diffusion coefficient $D \approx 10^{-6}\frac{cm^2}{s}$) [2].
Modifying the system's free parameters $D_c, \chi, \delta, D_m, \mu_3, \lambda$ gives us:

$$d_c = \tfrac{D_c}{D}, \quad \gamma = \chi\tfrac{e_0}{D}, \quad \eta = \tau m_0\delta, \quad d_m = \tfrac{D_m}{D}, \quad \alpha = \tau\mu_3\tfrac{c_0}{m_0}, \quad \beta = \tau\lambda.$$

with D being the aforementioned reference chemical diffusion coefficient.
These modifications make the new system of coupled partial differential equations, where the tildes are dropped and we assume t as τ for simplicities' sake, with also updated zero-flux boundary conditions:

$$\frac{\partial c}{\partial t} = d_c\Delta c - \gamma\nabla\cdot(c\nabla e) + \mu_1 c\left(1-\frac{c}{c_0}-\frac{e}{e_0}\right) \tag{6}$$
$$\frac{\partial e}{\partial t} = -\eta m e + \mu_2 e\left(1-\frac{c}{c_0}-\frac{e}{e_0}\right) \tag{7}$$
$$\frac{\partial m}{\partial t} = d_m\Delta c + \alpha c - \beta m \tag{8}$$

$$\zeta\cdot(-d_c\nabla c + c\gamma\nabla e) = 0 \tag{9}$$
$$\zeta\cdot(-d_m\nabla m) = 0 \tag{10}$$

where ζ is an outward unit normal vector.
In order to use the Finite Element Method we will change to the variational formulation. If we assume each species to be in the Hilbert space $H^1(\Omega)$, the variational formulation can be derived by multiplying with a test function φ_i, integrating over the domain Ω and use integration by parts and the Gauss theorem. This will give us a broader solution space and reduces the requirements of the solution regarding differentiability. With $(\cdot,\cdot)$ denoting the L^2-scalar product on Ω the following equation system results:

$$\left(\frac{\partial c}{\partial t},\varphi_c\right) = -d_c\left(\nabla c,\nabla\varphi_c\right) + \gamma\left(c\nabla e,\nabla\varphi_c\right) + \mu_1\left(c\left(1-\frac{c}{c_0}-\frac{e}{e_0}\right),\varphi_c\right) \tag{11}$$
$$\left(\frac{\partial e}{\partial t},\varphi_e\right) = -\eta\left(me,\varphi_e\right) + \mu_2\left(e\left(1-\frac{c}{c_0}-\frac{e}{e_0}\right),\varphi_e\right) \tag{12}$$
$$\left(\frac{\partial m}{\partial t},\varphi_m\right) = -d_m\left(\nabla m,\nabla\varphi_m\right) + \alpha\left(c,\varphi_m\right) - \beta\left(m,\varphi_m\right) \tag{13}$$

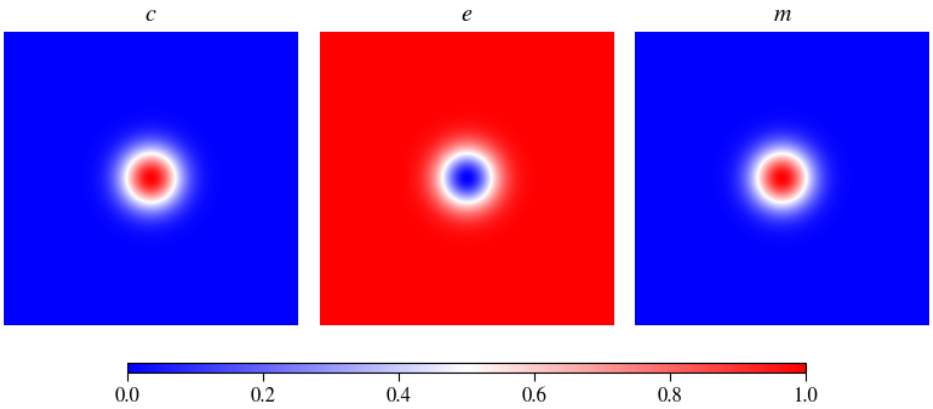

FIGURE 2. Visualization of the initial value distribution for an experiment in two space dimensions with a homogenous extracellular matrix

Non-dimensionalising our system of equations allows us to formulate the initial conditions in simple terms. Since our aim is to describe both homogenous as well as heterogenous extracellular matrix structures we have to respect this in regard to the initial conditions for the variable e.
Assuming that at dimensionless time $t = 0$ there is already a nodule of cells located at the center of the unit domain Ω we define the initial conditions for the tumour cell denisity as:

$$c(x, 0) = \exp(\frac{-(x - 0.5)^2}{\epsilon})$$

where for our experiments we used the value $\epsilon = 0.01$.
Assuming that these tumour cells have already produced an amount of matrix-degrading enzymes, we can define the inital conditions for the variable m the same way as the tumour cells were:

$$m(x, 0) = 0.5c(x, 0) = 0.5 \exp(\frac{-(x - 0.5)^2}{\epsilon})$$

Considering the initial strucutre of the extracellular matrix we suppose that the tumour cells have already degraded some of the extracellular matrix, especially at the center where the tumour cells are located. Furthermore we have to differentiate now between homogenous and heterogenous extracellular matrix structure. If the ECM has a homogenous structure, which means that it is evenly distributed in space we set its initial value as:

$$e(x, 0) = 1 - 0.5c(x, 0)$$

Figure 2 shows a 2D plot of the initial conditions using the homogenous extracellular matrix structure.
When we now assume a heterogenous ECM strucuture the initial conditions change to:

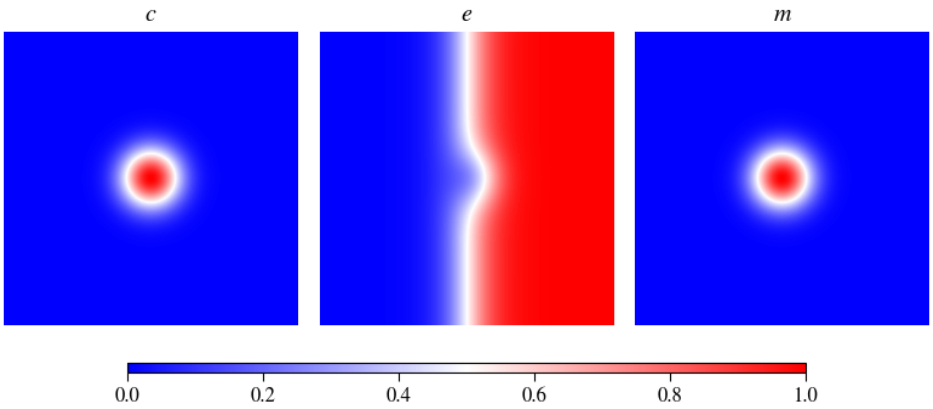

FIGURE 3. Visualization of the initial value distribution for an experiment in two space dimensions with a heterogenous extracellular matrix

$$e(x,0) = 1 - 0.5c(x,0)$$

In figure 3 these change of structure is clearly shown in the middle plot, where red inidcates that only on the left side there are extracellular matrix molecules.

4 Experiments and Results

All experiments that consider the ECM to be homogenous start with the same initial values as seen in figure 2. Experiments observing the effects of a heterogenous ECM use different initial values, as seen in figure 3.
Solving the numerical model HiFlow^3 will be used with the weak form given with equations 11 - 13. To evaluate the results of the numerical simulation ParaView [9] is used, producing informative plots to compare the evolution of the simulation in time. For this we rely on the tool Plot Over Line to give results for the three variables of tumour cell density, extracellular matrix density and matrix-degrading enzymes concentration.
This work starts with replicating numerical simulations done by other papers in higher dimensions. Since there were only 1D simulations done previously, the model will be adjusted in such a way, that the Plot Over Line graphs mimick the plots given by the previous experiments. This will serve two purposes, first it will verify a correct implementation of the model and second this will give us a starting point by which we can vary the parameters, investigating the phenomena this model exhibits.
We will start with examining 2D experiments with homogenous ECMs, using our model with the parameters μ_1 and μ_2 both set to zero, considering a case with no proliferation of tumour cells and no renewal of the extracellular matrix molecules, after this we will introduce proliferation and renewal, Incorporating μ_1 and μ_2 into the variation. Considering 3D experiments we will do a slimmer replication and parameter analysis due to the immense computational effort. After examining the model with a homogenous ECM initial condition we will move on to look at a case considering a heterogenous ECM in 2D.
Looking at the parameter estimates from [2] to non-dimensionalise the time, we see that with $L \in [0.1cm, 1cm]$ and $D \approx 10^{-6}\frac{cm^2}{s}$, $\tau = \frac{L^2}{D}$ would give us a big temporal range, $\tau_{min} = 1000s$ and $\tau_{max} = 1000000s$ in which the simulations take place. However using estimates taken from [10] and [5] for the length scale, with $L = 0.2cm$ gives us a concrete value for our non-dimensional time, $\tau = 40000s$, from now on t will stand as replacement for τ for simplicity reason.
Since Anderson et al. don't specify their exact value used for L, we needed to determine appropriate configurations for dt used in our simulation to get comparable results. We used a timestep of $dt = 0.01$ which corresponds to $400s$ and let the simulations run for a dimensionless time of $t = 8$ corresponding to $320000s = 88\ days$. Looking at the results below we found that for every unit of time in Anderson et al's experiments, in our experiements $t = 0.4$ have passed.
Another challenge are the diffusion coefficients, since they are dependent on the dimension we are in, we have to find our own estimates as a baseline value.
For each stage of experiments we will use a set of baseline parameters, which will be evaluated experimentally, and from there vary one or more parameter at a time to get an overview of their effects.
For all the plots of the experiments the red curve indicates the tumour cell density, the blue curve the ECM density and the green curve the MDE concentration. In all of the experiments we used the value of $\epsilon = 0.01$ to match the inital conditions from [2] and [11].

$d_c = 5e-4$ test 1e−10 test $5 \cdot 10^{-4}$

4.1 Two dimensional Results without Proliferation and Renewal

Figure	Linestyle	d_c	γ	μ_1	η	μ_2	d_m	α	β
4	——	$1 \cdot 10^{-3}$	0.005	0	10	0	$1 \cdot 10^{-3}$	0.1	0
5	—·—	$1 \cdot 10^{-3}$	0.005	0	10	0	$1 \cdot 10^{-3}$	0.2	0
5	·····	$1 \cdot 10^{-3}$	0.005	0	10	0	$1 \cdot 10^{-3}$	0.3	0
5	——	$1 \cdot 10^{-3}$	0.005	0	10	0	$1 \cdot 10^{-3}$	0.35	0
5	- - - -	$1 \cdot 10^{-3}$	0.005	0	10	0	$1 \cdot 10^{-3}$	0.4	0
6	—·—	$1 \cdot 10^{-3}$	0.005	0	10	0	$1 \cdot 10^{-3}$	0.3546	0
6	·····	$1 \cdot 10^{-4}$	0.005	0	10	0	$1 \cdot 10^{-3}$	0.3546	0
6	——	$5 \cdot 10^{-4}$	0.005	0	10	0	$1 \cdot 10^{-3}$	0.3546	0
6	- - - -	$1 \cdot 10^{-5}$	0.005	0	10	0	$1 \cdot 10^{-3}$	0.3546	0
7	—·—	$5 \cdot 10^{-5}$	0.005	0	10	0	$1 \cdot 10^{-3}$	0.3546	0
7	·····	$5 \cdot 10^{-4}$	0.0055	0	10	0	$1 \cdot 10^{-3}$	0.3546	0
7	——	$5 \cdot 10^{-4}$	0.006	0	10	0	$1 \cdot 10^{-3}$	0.3546	0
7	- - - -	$5 \cdot 10^{-4}$	0.007	0	10	0	$1 \cdot 10^{-3}$	0.3546	0
8	——	$5 \cdot 10^{-4}$	0.0055	0	10	0	$1 \cdot 10^{-3}$	0.3546	0
9	—·—	$5 \cdot 10^{-4}$	0.0055	0	10	0	$1 \cdot 10^{-3}$	0.3546	0
9	——	$1 \cdot 10^{-3}$	0.0055	0	10	0	$1 \cdot 10^{-3}$	0.3546	0
9	·····	0.1	0.0055	0	10	0	$1 \cdot 10^{-3}$	0.3546	0
10	·····	$5 \cdot 10^{-4}$	0.002	0	10	0	$1 \cdot 10^{-3}$	0.3546	0
10	——	$5 \cdot 10^{-4}$	0.008	0	10	0	$1 \cdot 10^{-3}$	0.3546	0
10	- - - -	$5 \cdot 10^{-4}$	0.01	0	10	0	$1 \cdot 10^{-3}$	0.3546	0
11	——	$5 \cdot 10^{-4}$	0.1	0	10	0	$1 \cdot 10^{-3}$	0.3546	0
12	——	$5 \cdot 10^{-4}$	0.1	0	10	0	$1 \cdot 10^{-3}$	0.3546	0
13	·····	$5 \cdot 10^{-4}$	0.0055	0	2	0	$1 \cdot 10^{-3}$	0.3546	0
13	——	$5 \cdot 10^{-4}$	0.0055	0	12	0	$1 \cdot 10^{-3}$	0.3546	0
13	·····	$5 \cdot 10^{-4}$	0.0055	0	20	0	$1 \cdot 10^{-3}$	0.3546	0
14	·····	$5 \cdot 10^{-4}$	0.0055	0	10	0	0.00001	0.3546	0
14	——	$5 \cdot 10^{-4}$	0.0055	0	10	0	0.001	0.3546	0
14	·····	$5 \cdot 10^{-4}$	0.0055	0	10	0	0.1	0.3546	0
15	·····	$5 \cdot 10^{-4}$	0.0055	0	10	0	$1 \cdot 10^{-3}$	0	0
15	——	$5 \cdot 10^{-4}$	0.0055	0	10	0	$1 \cdot 10^{-3}$	0.6	0
15	·····	$5 \cdot 10^{-4}$	0.0055	0	10	0	$1 \cdot 10^{-3}$	1.0	0
16	·····	$5 \cdot 10^{-4}$	0.0055	0	10	0	$1 \cdot 10^{-3}$	0.3546	0.1
16	——	$5 \cdot 10^{-4}$	0.0055	0	10	0	$1 \cdot 10^{-3}$	0.3546	0.01
16	·····	$5 \cdot 10^{-4}$	0.0055	0	10	0	$1 \cdot 10^{-3}$	0.3546	0.005
17 - left	·····	0.00005	0.001	0	10	0	$1 \cdot 10^{-3}$	0.3546	0
17 - left	——	0.00005	0.01	0	10	0	$1 \cdot 10^{-3}$	0.3546	0

continued on next page

Figure	Linestyle	d_c	γ	μ_1	η	μ_2	d_m	α	β
17 -right	·····	0.1	0.001	0	10	0	$1 \cdot 10^{-3}$	0.3546	0
17 -right	——	0.1	0.01	0	10	0	$1 \cdot 10^{-3}$	0.3546	0
18 - left	·····	$5 \cdot 10^{-4}$	0.0055	0	2	0	0.0000000001	0.3546	0
18 - left	——	$5 \cdot 10^{-4}$	0.0055	0	20	0	0.0000000001	0.3546	0
18 -right	·····	$5 \cdot 10^{-4}$	0.0055	0	2	0	0.1	0.3546	0
18 -right	——	$5 \cdot 10^{-4}$	0.0055	0	20	0	0.1	0.3546	0
19 - left	·····	$5 \cdot 10^{-4}$	0.0055	0	10	0	$1 \cdot 10^{-3}$	0.1	0.005
19 - left	——	$5 \cdot 10^{-4}$	0.0055	0	10	0	$1 \cdot 10^{-3}$	0.1	0.1
19 -right	·····	$5 \cdot 10^{-4}$	0.0055	0	10	0	$1 \cdot 10^{-3}$	1.0	0.005
19 -right	——	$5 \cdot 10^{-4}$	0.0055	0	10	0	$1 \cdot 10^{-3}$	1.0	0.1
20 - left	·····	$5 \cdot 10^{-4}$	0.0055	0	10	0	0.0000000001	0.1	0.005
20 - left	——	$5 \cdot 10^{-4}$	0.0055	0	10	0	0.0000000001	0.1	0.1
20 -right	·····	$5 \cdot 10^{-4}$	0.0055	0	10	0	0.0000000001	1.0	0.005
20 -right	——	$5 \cdot 10^{-4}$	0.0055	0	10	0	0.0000000001	1.0	0.1
21 - left	·····	$5 \cdot 10^{-4}$	0.0055	0	10	0	0.1	0.1	0.005
21 - left	——	$5 \cdot 10^{-4}$	0.0055	0	10	0	0.1	0.1	0.1
21 -right	·····	$5 \cdot 10^{-4}$	0.0055	0	10	0	0.1	1.0	0.005
21 -right	——	$5 \cdot 10^{-4}$	0.0055	0	10	0	0.1	1.0	0.1

TABLE 1. Overview of all experiments conducted for the model without proliferation and renewal producing 2D output

Table 1 shows all the experiments done in two space dimensions using the model without proliferation or renewal. You can see the figure and the linestyle to verify exactly which experiment uses which values.

4.1.1 Replicating results

We will start with replicating the experiment from Anderson et al.[2], Figure 4, trying to make our curves fit the results of their experiment.

We start with the same parameters as in Anderson et al's first one dimensional experiment: $d_c = 1 \cdot 10^{-3}, d_m = 1 \cdot 10^{-3}, \gamma = 0.005, \eta = 10, \alpha = 0.1, \beta = 0, \mu_1 = 0, \mu_2 = 0$. Figure 4 shows these results for four different points in time. Since our experiments are preformed in two dimensions you can see on the left side the two dimensional plots of the tumour cell density and on the right side you can see plots produced by applying the Plot Over Line tool confiugrated like described in the section **??**, where there is not only the tumour cell density visible but also the matrix-degrading enzymes concentration and the extracellular matrix concentration. We choose these points in time, because we used a different timescale than Anderson et al. and as you will later see, our time points capture the effects that can be observed studying their results quite well, which implies that for every time step Anderson et al. did we had to do 4. The problem with the two dimensional plots is that as you can see overlaying the different variables of tumour cell density, MDE concentration and ECM concentration, makes the plots unreadable, so you

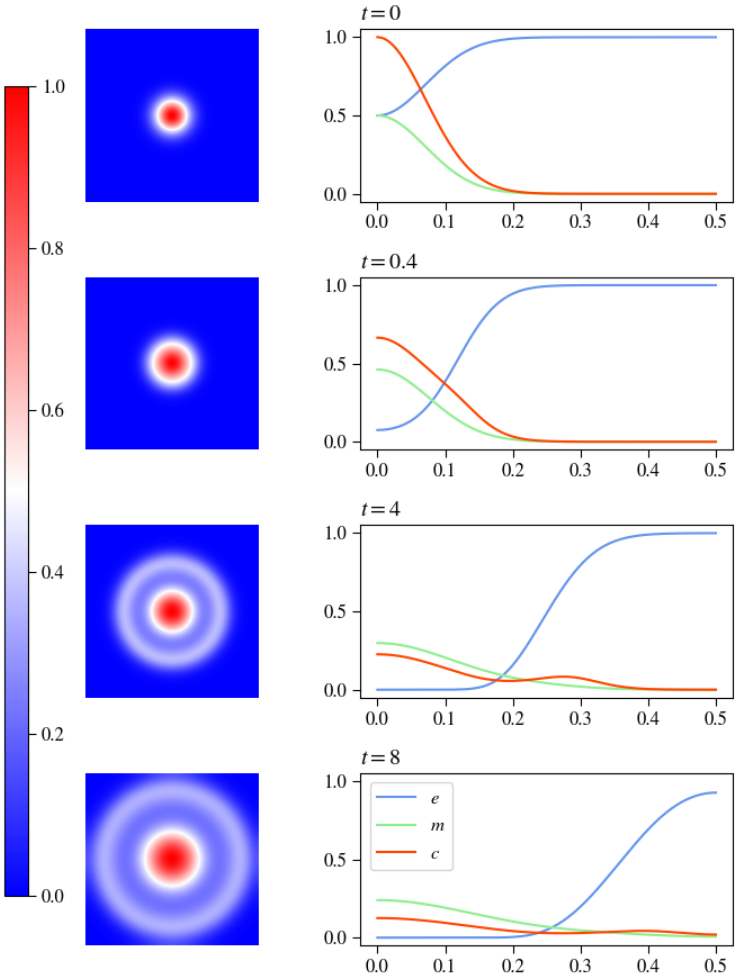

FIGURE 4. Results using Anderson et al's parameters, left side 2D tumour cell density plots, right side results produced by applying the Plot Over Line tool

can only show one at a time, additionally to this it is harder to estimate values for c, e and m at different locations in space and time. These problems are solved using the Plot Over Line tool, as you can see in the plots of figure 4 on the right side the curves for the three variables are clearly distinguishable and we can estimate their values spacially and temporarily better. This is why for most experiments we resort to using only the results produced by the Plot Over Line method instead of full 2D simulation images, this makes evaluating and comparing the respective experiments a lot easier and still captures all occuring effects.
Starting from the inital values at $t = 0$ we see that after four time steps a very small secession is starting to form for the tumour cell density at $x \approx 0.1$. Diffusion and Haptotaxis have stretched the curve for the tumour cells along the x-axis as did diffusion for the MDEs. The ECM has been visibly degraded at the origin, being still fully present in outer regions exceeding $x \approx 0.2$.
The next image shows the simulation after 0.4 timesteps; we see that the secession of the tumour cell concentration of the previous point in time has been propagated to form a small hill at the leading edge of the tumour cells invading the surrounding tissue, this effect is due to the haptotatic influence, which pulls the tumour cells further into the accessible area towards higher values of $\nabla(c\nabla e)$, creating a seperation for the tumour cells, where the other part is still oriented towards the origin. The MDEs also continue their diffusion into the area, degrading the ECM in their wake.
In the last image, after 8 simulation time steps, we see that as well the hill that has formed at the leading edge of the tumour cells as well as the concentration of tumour cells at the origin, have flattened visibly and striving to take on a constant concentration throughout space, though we can still clearly distinguish both areas. If we were to look at the simulation at later points in time, the curve will flatten even more, since with more time the ECM will be further degraded and therefore the haptotactic flux coefficient γ will lose its significance, leaving the movement of the tumour cells to diffusion only and spreading them constantly along the x-axis. The curve for the MDEs will also flattened due to diffusion,with the MDEs degrading the rest of the extracellular matrix molecules decrease their concentration further and the MDE concentration will increase over time due to no limiting factors in this experiment and on-going production contributed by the tumour cells c.
Comparing 4 to figure 1 in [2], we can see major differences. The first image showing $t = 0$ looks the same, which confirms that both experiments start with the same initial values condition. In the images showing the simulation at the second time checkpoint we see that though the tumour concentration and ECM density values are approximately the same, the MDE concentration is slightly lower in our experiment, which will get more pregnant in the later images. The unevenness having formed at the leading edge of the tumour cell concentration is also slightly smaller. The differences in the third image are more striking, both c and m have considerably lower concentrations, yet the ECM value looks is very similar.
In our case the diffusion and haptotatic pull of the tumour cells has shown to be too stong making the invasion process into the tissue happen too fast. The last time checkpoints strengthens our findings, showing the same behaviour with ECM being approximately the

same, tumour cell density and MDE concentration being clearly lower in our experiment and invasion of tissue happening too fast, leaving the lump at the origin $x = 0$ too small. This first of all confirms the initial supposition that with changing the dimension for the simulations the results also vary. We will now adjust the parameters iteratively to make the results using two dimensions mimick the results from Anderson et. al as closely as possible. For this we will start with varying the MDE production coefficient α, to get higher concentration values for the MDEs, and change the diffusion as well as haptotaxis coefficients of the tumour cells d_c and γ, to adjust the motitlity of the tumour cells and therefore also influence the invasion speed of them into the surrouding tissue.

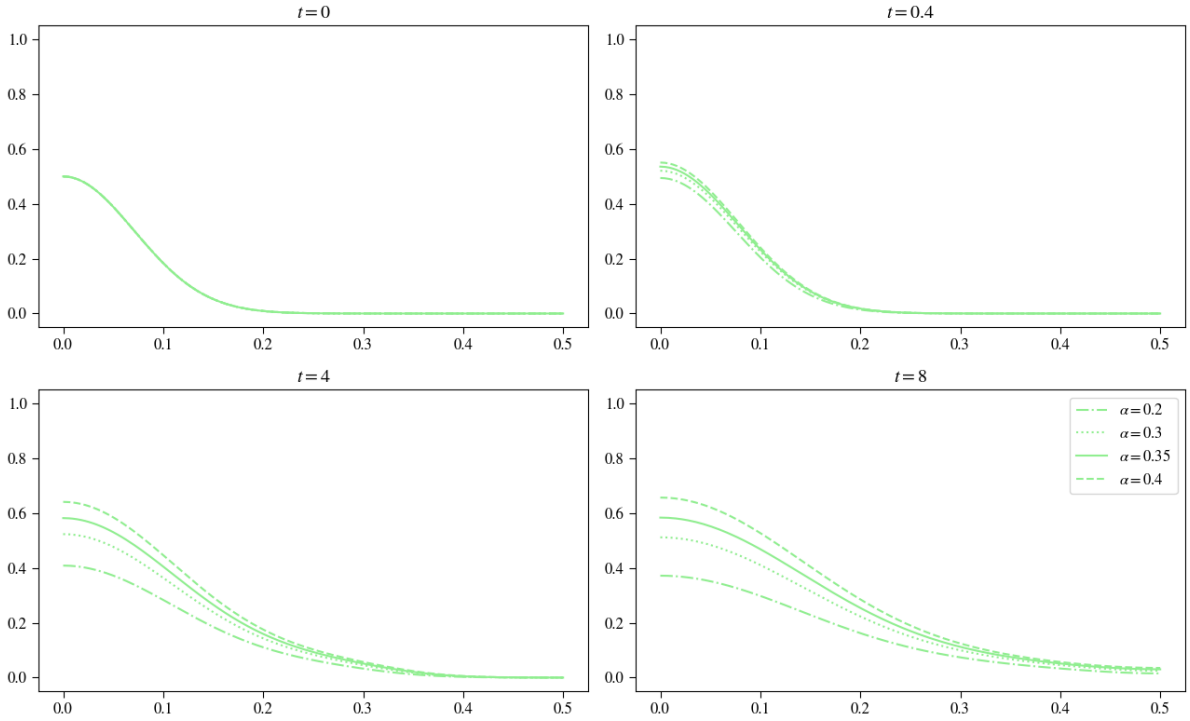

FIGURE 5. Results using Anderson et al's parameters but varying α using the Plot Over Line tool

Figures 5, 6 and 7 show these comparisons of the parameters α, d_c and γ. Comparing different values for α and their effect on the curve of the MDE concentration, shows in figure 5 that, especially looking at the later points in time $t = 4$ and $t = 8$, with values for α between 0.3 and 0.4 we will get a good approximation. The values of the original paper for the MDEs are for $t = 4$ approximately 0.6 at $x = 0$ and for $t = 8$ about 0.7 at the same point in space. With a value $\alpha = 0.35645$ we got the best results regarding the MDE concentration.
Looking at d_c we chose a value of $d_c = 5 \cdot 10^{-4}$. Using values below 0.00001 will result in numerical instabilities and results that are not longer useable. For γ we made a slight adjustment upwards to $\gamma = 0.0055$ to have a little bit more pull on the tumour cells outward, to match the invasion speed observed in the original paper.

These adjustments leave us with the final configuration for replicating the system with

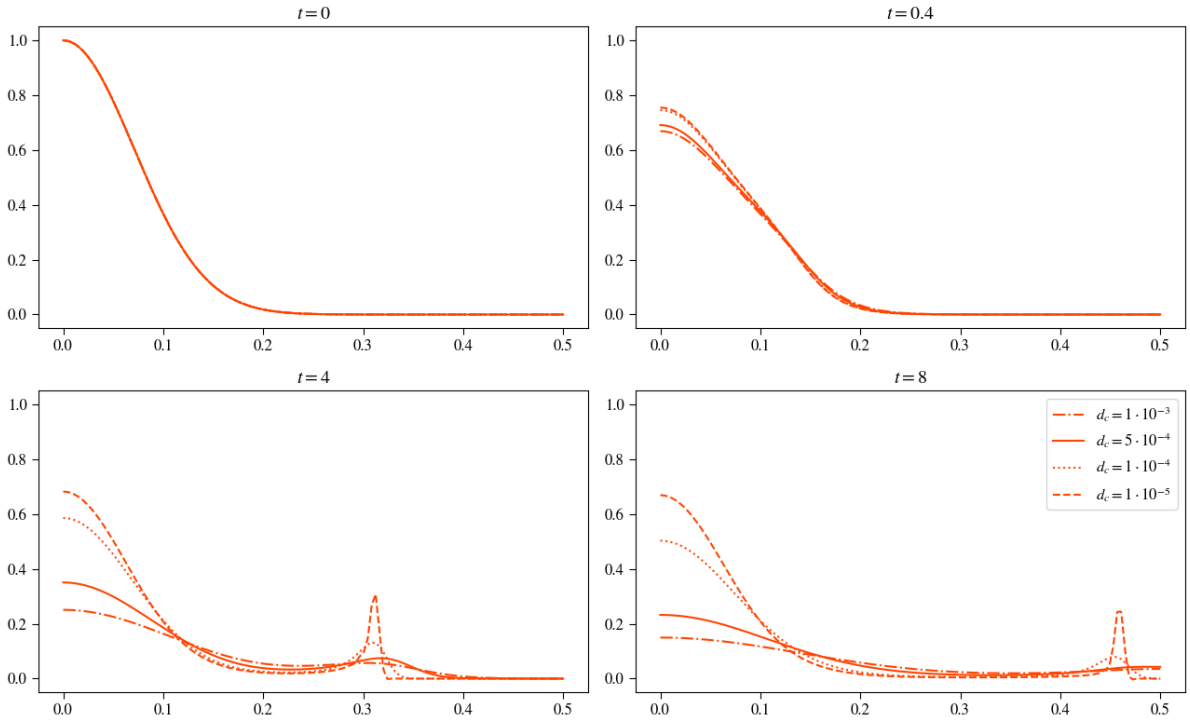

FIGURE 6. Results using Anderson et al's parameters but varying d_c using the Plot Over Line tool

the curves in figure 8 and the parameter settings also seen in the same figure. Comparing our final version with the original experiment we are trying to replicate we can see that in the second point in time, at $t = 0.4$ in our case, the values of the three curves at the $x = 0$ are nearly the same, and moving farther out along the x-axis the curves mimick each other quite well. In the original experiment the bump in the curve for the tumour concentration looks more pregnant, but this is due to the differing dimensions and the rescaling of the x-axis done in Anderson et al's experiment. The two later points in time confirm the similarity with having also nealy the same values for the three curves over the whole space domain.

4.1.2 Parameter Analysis

Mathematical Intuition of the three curves and how the parameters interact

From the replicated results shown in figures 8, we saw that if we vary certain parameters one at a time the results also vary strongly. Therefore we are now going to have a look at how changing one parameter affects the output of the whole system. For this we assume the parameter values of the replicated results to be our set of baseline parameters, from there in each experiment only one parameter is changed at first, later we will also perform cross variations, where more than one parameter is changed at a time, to see how they interact and change the results.

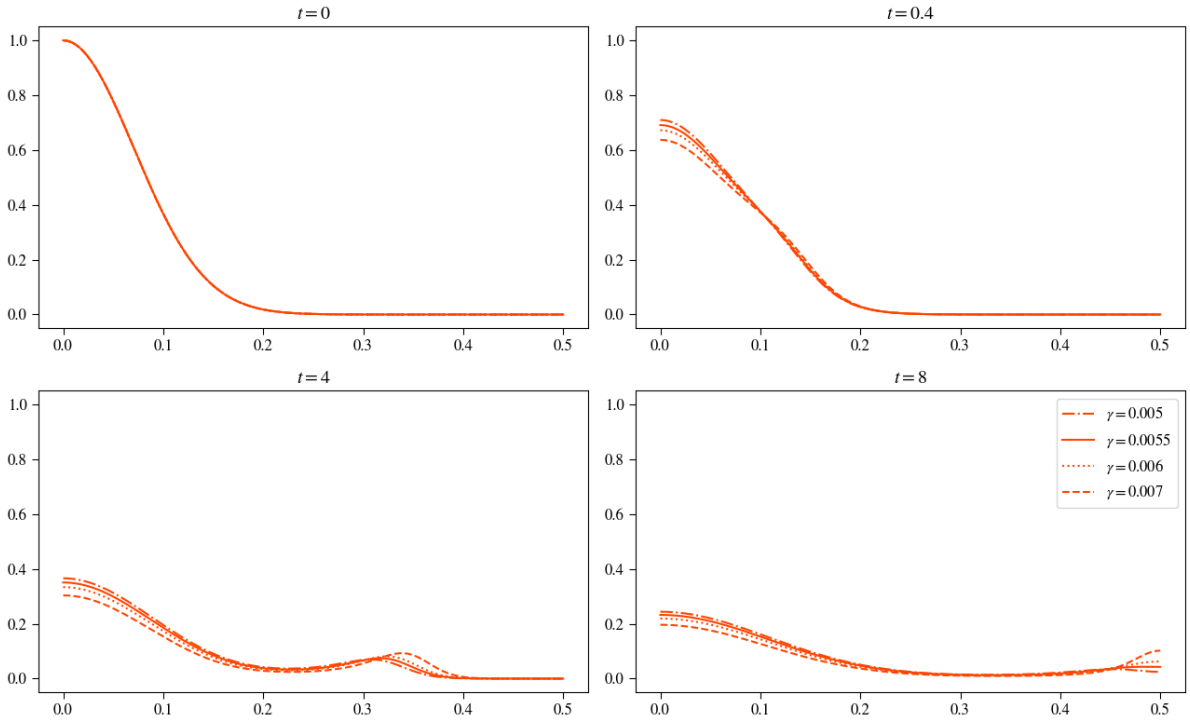

FIGURE 7. Results using Anderson et al's parameters but varying γ using the Plot Over Line tool.

d_c Variation

The parameter describes the diffusion of the tumour cells. We assume this parameter to be evenly distributed with $d_c \sim U[0.00005, 0.1]$, as both lower and higher values for diffusion will distort the results and make them unusable.
The mathematical intuition is that if we will decrease d_c we will see the effects of γ taking over in the simulation results for the c curve, meaning that the tumour cells are more likely to drift outward as one lump of cells and leavoe only a little concentration at the origin. On the other hand if we increase d_c the effects of haptotaxis will diminish, the tumour cells will be subject to higher diffusion distributing them more evenly into the tissue, there will be less of a secession that is seperated from the main lump of cells, which will stay at the origin. Looking at the experiments in figure 9, we can see these assumptions met. The smaller d_c gets the higher the influence of γ will be and vice versa. Considering the tumour cell denisty curves shown in red, we can after already $t = 0.4$ timesteps see big differences. For both lower values of d_c we see the main lump of cells starying at the center, but between these two we can already see the tendency of the curve describing the experiment for $d_c = 1 \cdot 10^{-3}$ to invade faster into the tissue. In this regard the curve decribing the highest value of diffusion has already taken on a constant distribution of tumour cells in space. The differences in the tumour cells distributions influence the curves for the concentration of the matrix-degrading enzymes, with increasing d_c the MDEs have also spread furhter into the space. Concerning the degradation of the

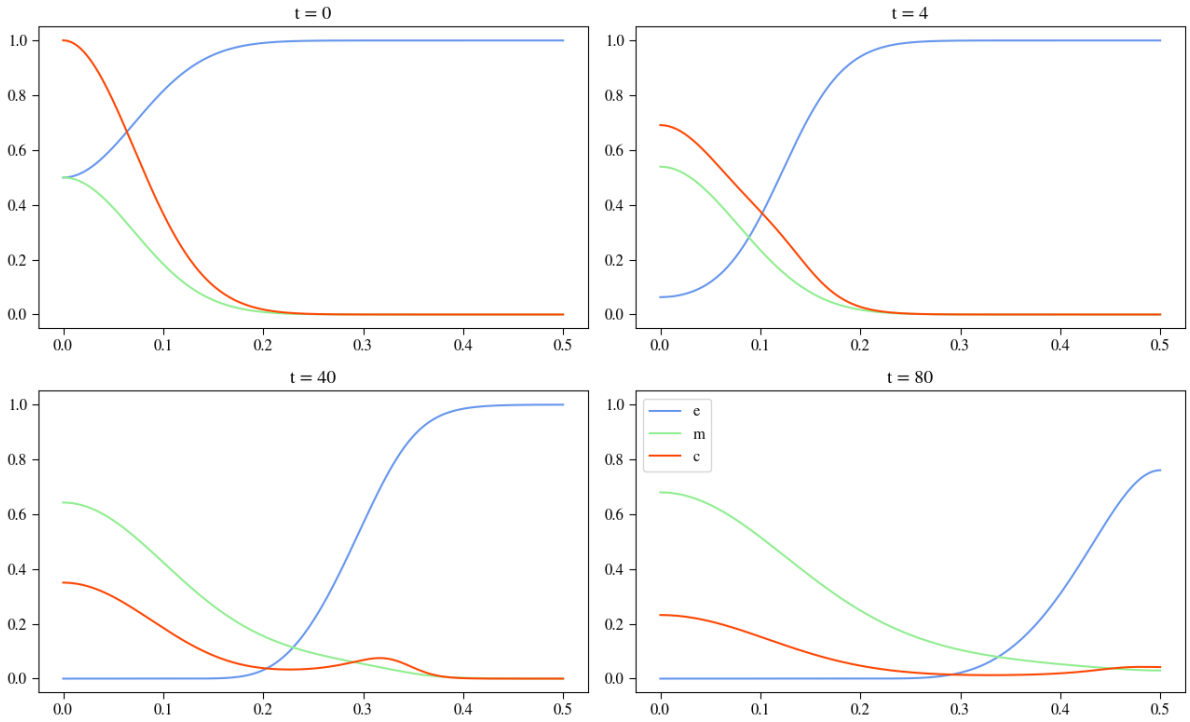

FIGURE 8. Results of using the parameters as described, this experiment will be used as the basecase to compare further experiments to ragarding the model without proliferation and renewal

ECM we see at this point in time only little deviations between varying d_c, though we can already observe that with rising d_c the ECM will be degraded slower.
Looking at the next checktpoint in time at $t = 4$ we see the observed effects intensifying. The curve of the tumour cells showing the experiment for $d_c = 0.1$ stayed in its constant distribution, not visibly and numerically changing, for the other two curves showing the smaller values of diffusion we see the effect of haptotaxis here clearly, with the tumour cells dividing into two main lumps of cells, where one stays at the origin and the other invades space in a higher pace. We see this behaviour increase as we decrease d_c. Coming back to our initial assumption that effects of haptotaxis increase as we decrease d_c we see this again confirmed. For the MDE curves we can observe the same effects as in the previous image at $t = 0.4$; the curve of experiment with the slowest diffusion has the strongest concentration of MDEs at the center, this concentration decreasing with increasing diffusion. It is interesting to note that the area of the MDE concentrations strongly differ. Yet we see that these differences in total matrix-degrading enzymes does not strongly influence the degradation of the extracellular matrix. On the contrary the dotted curve has the lowest value of total matrix-degrading enzymes, thought the ECM degradation happens the faster and more evenly than the other two, which implies that there is only a small concentration of MDEs needed to efficiently degrade the ECM and that higher diffusion of the tumour cells causes a faster ECM degradation.
The last images verifies the aforementioned effects once again to conclude that with in-

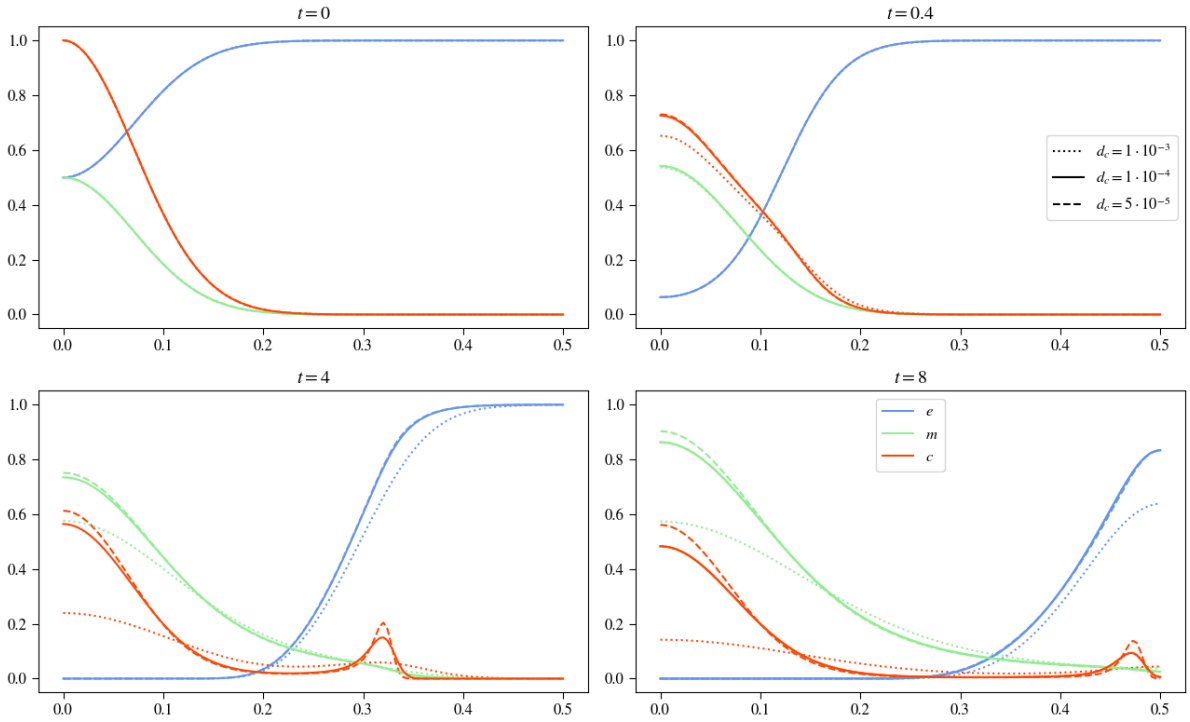

FIGURE 9. Results of varying d_c in the basecase parameter set, keeping the other parameters constant, using the Plot Over Line tool

creasing d_c we see a faster invasion of the tissue, due to accellerated diffusion, though with decreasing effects of haptotaxis. The higher the values for the diffusion factor the more evenly the spreading of the tumour cells will happen with less of a secession forming that seperates the tumour cells into two main lumps. The total MDE concentration in space diminishes with increasing d_c though this shows countering effect on ECM degradation, with the ECM degradation also accellerating with increasing diffusion.

γ Variation

γ describes the effects of haptotaxis, it is assumed that it is evenly distributed in $\gamma \sim U[0.001, 0.01]$, values exceeding this region will as described later produce results that lose their biological meaning.Inspecting the effects of γ we can assume the countering effects as for d_c; if we select higher values for γ the effects of haptotaxis, creating a secondary lump of cells that is being pulled faster into the tissue, to increase, taking lower values for γ, the diffusion will be superior factor for the tumour cell motility, which will result in no secession at the leading edge of the tumour cell's tissue invasion. The experiments, described in figure 10 verify the expected behaviour. After $t = 0.4$ we already see clear changes for varying γ, the higher γ is set, the more of a secession for the tumour cells is observable, that will later from the secondary lump. The lowest value for γ, undercutting the one for the basecase, shows no signs of a leading edge forming that invades the tissue seperately. The other two variables show little deviation with varying γ at this point in

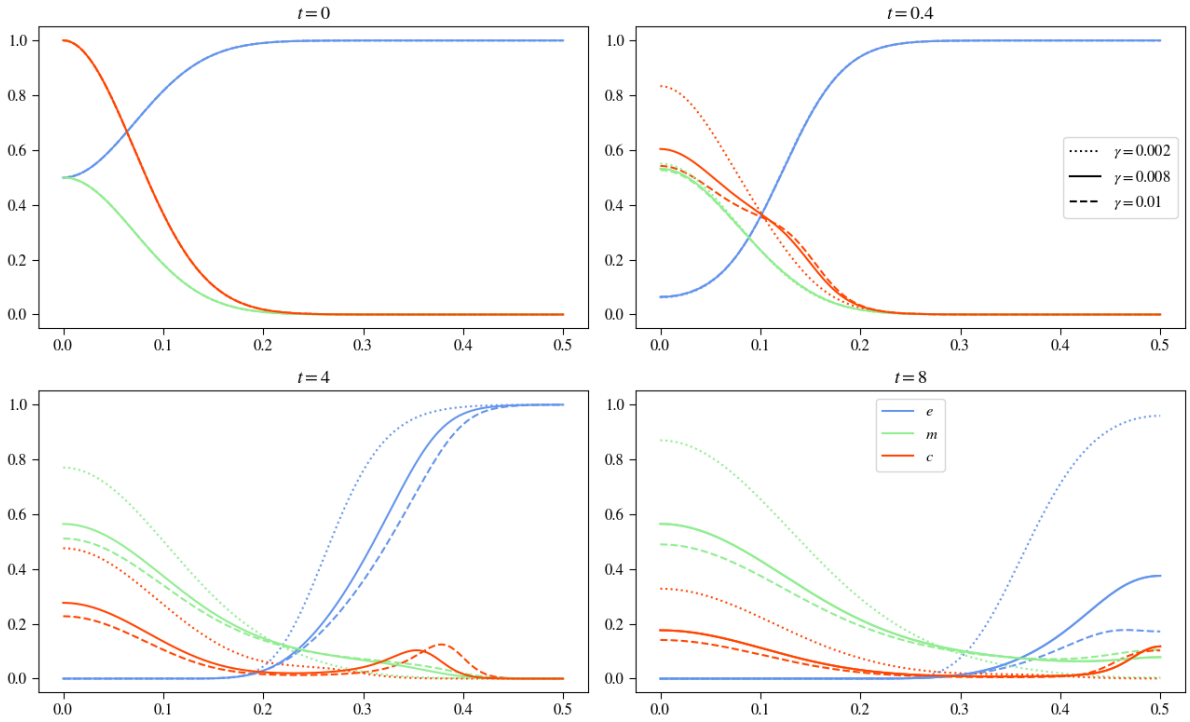

FIGURE 10. Results of varying γ in the basecase parameter set, keeping the other parameters constant, using the Plot Over Line tool

time.

The next image shows the simulation after $t = 4$ timesteps and here we can clearly see changes in all three variables. Whilst the tumour cell density for the values of 0.008 and 0.01 differ slightly by the amount of cells that are left at the origin and the distance they have already invaded the surrouding tissue, the curve for the value $\gamma = 0.002$ does not even show a leading edge, that is being pulled by haptotaxis into the tissue, this causes the tumour cells to stay centered around $x = 0$, resulting in a higher denisty of cells there compared to the restuls of the other experiments. With increasing γ the invasion speed also increases, as the dashed line for the tumour cell density shows. For the MDE curve we also observe that the lower γ is the more of the concentration is at the origin, decreasing outwards. This is due to the tumour cells for the lowest γ value behaves the same, and as they are produbing the matrix-degrading enzymes. The ECM concentration shows similiar behaviour as the MDE concentration does, with increasing γ, the ECM is faster and more evenly degraded, due to the faster invasion of the tissue, the production of matrix-degrading enzymes happens also in regions farther away from the center. As we saw varying d_c only little of MDE concentration is needed to efficiently degrade the extracellular matrix, therefore the ECM degradation process happens also faster here.

In the last image at $t = 8$ we see observations rom the previous points in time confirmed; the higher γ the faster the invasion pace of the tumour cells and the farhter out the MDE concentration has spread resulting in faster ECM degradation.

Out of curiousity we are going to take a step further and increase γ again by one potence,

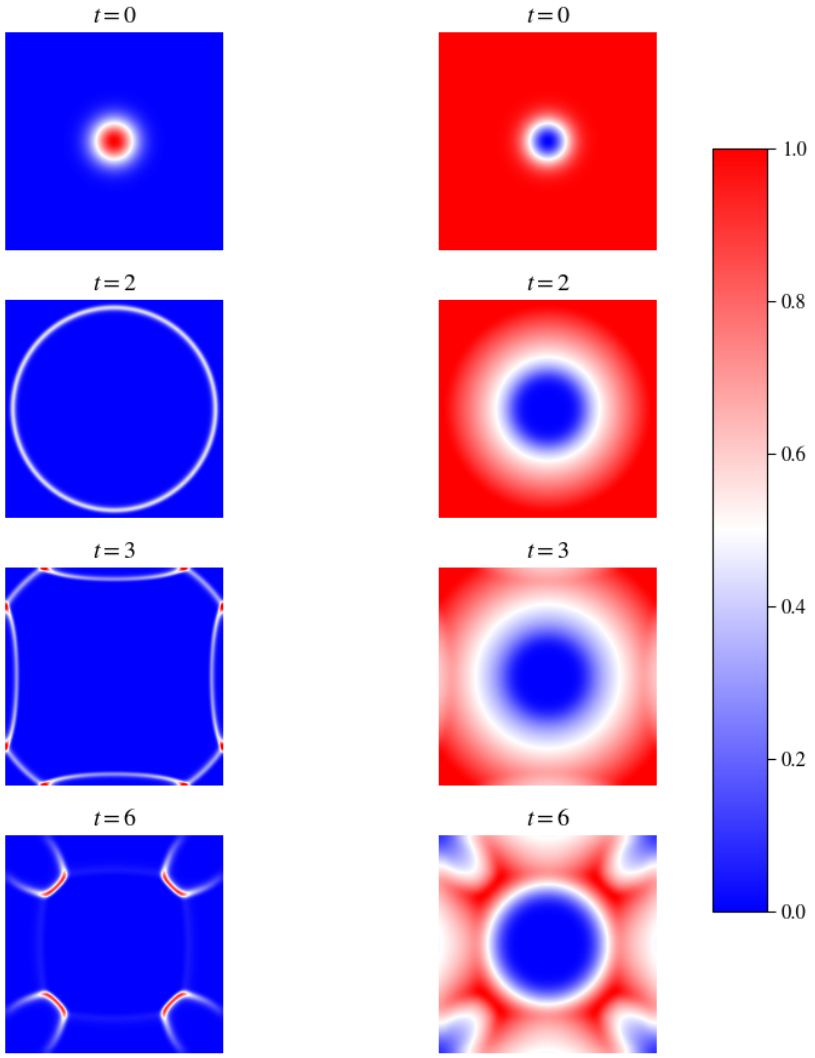

FIGURE 11. 2D plot of variation

to $\gamma = 0.1$. As previously observed the haptotatic effects pulling the cells into tissue increase, causing an even faster invasion pace and therefore spread of matrix-degrading enzymes, yet in this case the invasion pace of the tumour cells is so high, that before finishing the simulation we reach the square's border and the cells get reflected upon contact, due to the boundry conditions of our initial problem *insertreference*. Where we had radial symmetry assumed we are leaving it now, in figures 11 and **??** you can see at $t = 20$ already the border is reached and at $t = 30$ the cells have been reflected to move into the corners or inwards. In figure **??** you can especially well see that radial symmetry is left for this experiment, on the right side you see a Plot Over Line from the center of the simulation to one of the corner points, and see after $t = 30$ widely different results, on the left side the tumour cells have been reflected on the border whereas the tumour cell concentration described on the right side still invades further into the tissue, into the corner. But not only the tumour cell concentration along this new axis from the center

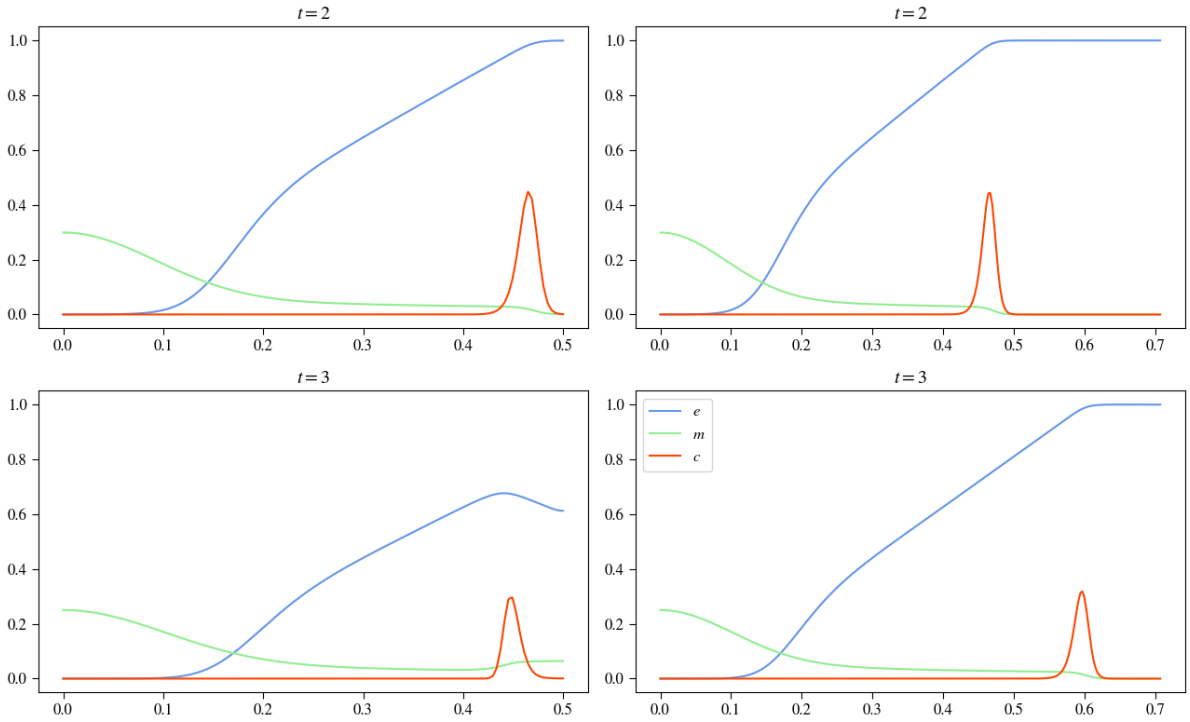

FIGURE 12. Plot OVer Line Comparison Gamma

to the corner points is being pulled into the corners, also the other tumour concentration in the area as well, as they are pulled into the direction where the ECM concentration is still strongest. On the right side of figure 11 at $t = 30$ you see this behaviour. To the fast invasion pace of the tumour cells the matrix-degrading enzymes have not been able to keep up, which leaves us with a situation where there is still a high concentration of extracellular matrix molecules left in the center of the simulation. This remaining ECM causes a movement of the tumour cells back towards the center, since those remaining ECM molecules there pull them back in, by haptotaxis. Though this behaviour makes no sense from a biological perspective, due to the boundry conditions of the system reflecting the movement, it is still interessting to investigate this case, from a numerical perspective. Though the intuition is met that with increasing γ the invasion pace of the tumour cells and matrix-degrading enzymes also rises, we get unexpected behaviour with the tumour cells invasion being so fast that they get reflected at the border of the unit cube and pulled into the corners and from there back in by not degraded ECM. Further increasing γ will only increases this behaviour and make this osicilating process even stonger.

η Variation

The parameter η controls the degradation process of the extracellular matrix moluecules, which can therefore heavily influence the produced results, as the ECM plays a crucial role also in regard to the motility of the tumour cells. We assumed the paramter η to be evenly distributed in $\eta \sim U[0, 20]$. Though it is a neglectable case that the ECM

cannot be degraded, by setting $\eta = 0$, it is still interesting to a look at how this affects the simulation. In reality it would certainly make more sense to define this paramter as being larger than zero.
With increasing η the ECM is faster degraded and therefore might provoke a faster invasion of the tissue. The higher η is the less MDEs are needed to degrade.
Inspecting the results in figure 13 we see our intuition confirmed. Across all images you

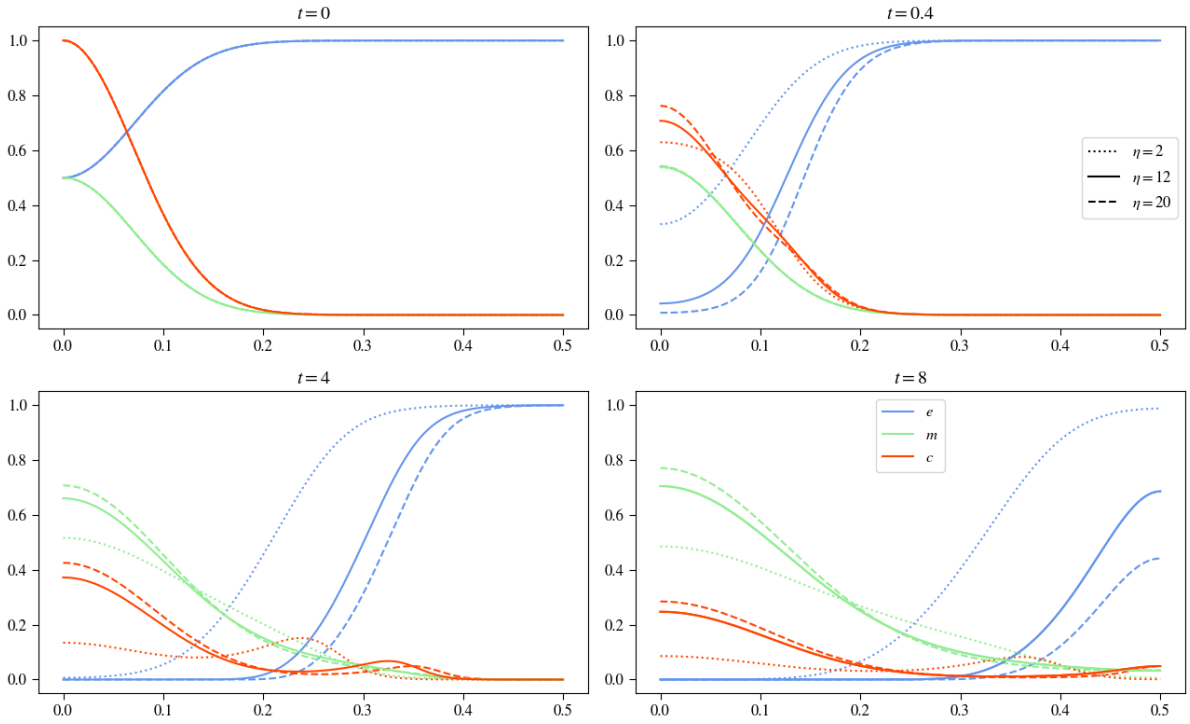

FIGURE 13. Plots show results for varying η whilst keeping the other parameters constant, in the images you can see the effects of $\eta = 20$ in the dashed curve, $\eta = 0$ in the dotted curve and $\eta = 12$ in the solid line.

can see that with $\eta = 0$, the dotted curves, the curve describing the ECM concentration stays constant, as $\frac{\partial e}{\partial t} = 0$ implies and due to this ∇e also stays constant in time, which plays an important role, modelling haptotaxis. This in turn causes the haptotatic term $\nabla(c\nabla e)$ to create a slowly changing

inspect – haptotactic

This causes the tumour cell density to create no hill at the leading edge invading the tissue, since the haptotatic effect of the pull of the ECM is limited to happen with a distance of $x = 0.2$. At the two later points in time the tumour cells for the experiment with $\eta = 0$ take on a distribution with only one maximum located beneath where the value for $\delta c(\delta e)$ is highest, due to this point not changing much, the curve for c does neither. Due to the limited motitlity of the tumour cells they doe not invade the tissue at all. The curve for the MDEs also looks much different from the basecase, after increasing intially slightly at $t = 4$, the curve curve interestingly does not increase over this limit of 0.528, with the tumour cells invading the tissue the MDEs follow with their production as well.

Since the maximum of c does not drastically change after $t = 8$ the curve for the MDE continues increasing in this region as well, though not as strongly since the tumour cells concentration also diffuses over time. The solid curve describing $\eta = 12$ does not strongly differ from the base case, exhibiting the expected behaviour of a stem of cells splitting off the main bulk invading the tissue at a faster rate and after $t = 8$ having invaded the outer regions of the tissue as well. The curves for the MDEs and ECM follow the description of the basecase experiment. Increasing η to 20, the dashed line, the behaviour change is not so drastic comparing it to $\eta = 12$. Thoug the degradation of the ECM happens twice as fast, the resulting accellerated invasion pace of the tumour cells, is not this pregnant. Interesting is that the hill at the leading edge of the tumour cells is though farther out also smaller than for the previous experiment, this might be due to the accellerated invasion pace, the tumour cells leading hill is also stretched farther. The remaining lump of tumour cells at the origin has also taken on a higher value than the experiment for the solid line, reason for this could be that with the faster degradation the effects of haptotaxis have a bigger influence on regions that are farther away from the origin, which will leave the remaining cells at the origin more subject to diffusion, because of the faster degradation the tumour cells at $x = 0$ are a shorter time influenced by strong haptotatic pull, leaving more of them at the origin. Looking at the ECM concentration it has after $t = 8$ as expected more decreased than previous experiments varying η. The MDE concentration has at the origin where the tumour cell concentration is higher for $\eta = 20$ than for $\eta = 12$ also a higher concentration, moving farther out we can also see that in those regions it is slightly lower than for the experiment with $\eta = 12$, this only makes sense, since there the tumour cell density, producing the MDEs is not as strong. Overall we can see that with increasing η the ECM degrading process is accellerated and also the invasion pace, with the tumour cells we can observe that due to faster invasion the remaining cells at the origin have a higher concentration as for the basecase, yet the hill at the leading edge of the tumour cells is smaller and for the MDEs they mimick this behaviour with a larger concentration at the origin as the basecase though smaller concentration at the invasion edge of haptotaxis.

d_m Variation

d_m is describes the diffusion coefficient of the matrix-degrading enzymes and like for diffusion of the tumour cells we assume it to be evenly distributed with $d_m \sim U[0.00001, 0.1]$. Looking at the equations governing the system a faster diffusion of the MDEs into the tissue will cause a faster ECM degradation, since as seen in the experiment varying d_c only little concentration of the matrix-degrading enzymes is needed to efficiently degrade the ECM. Faster ECM degradation will reduce haptotatic effects on the tumour cells, since the pull of it diminishes, causing a slower invasion pace.
Inspecting the results in figure 14 we observe that in the second image after $t = 0.4$ for $d_m = 0.1$, as for varying the diffusion of the tumour cells, the matrix-degrading enzymes have taken on a constant distribution in space, which as the later point in time show does not change, only the concentration level will increase. This strongly affects the ECM concentration as well, after this short time the ECM has visibly differently than the other for the lower values of d_m. Though the overall ECM concentration at this point in time is

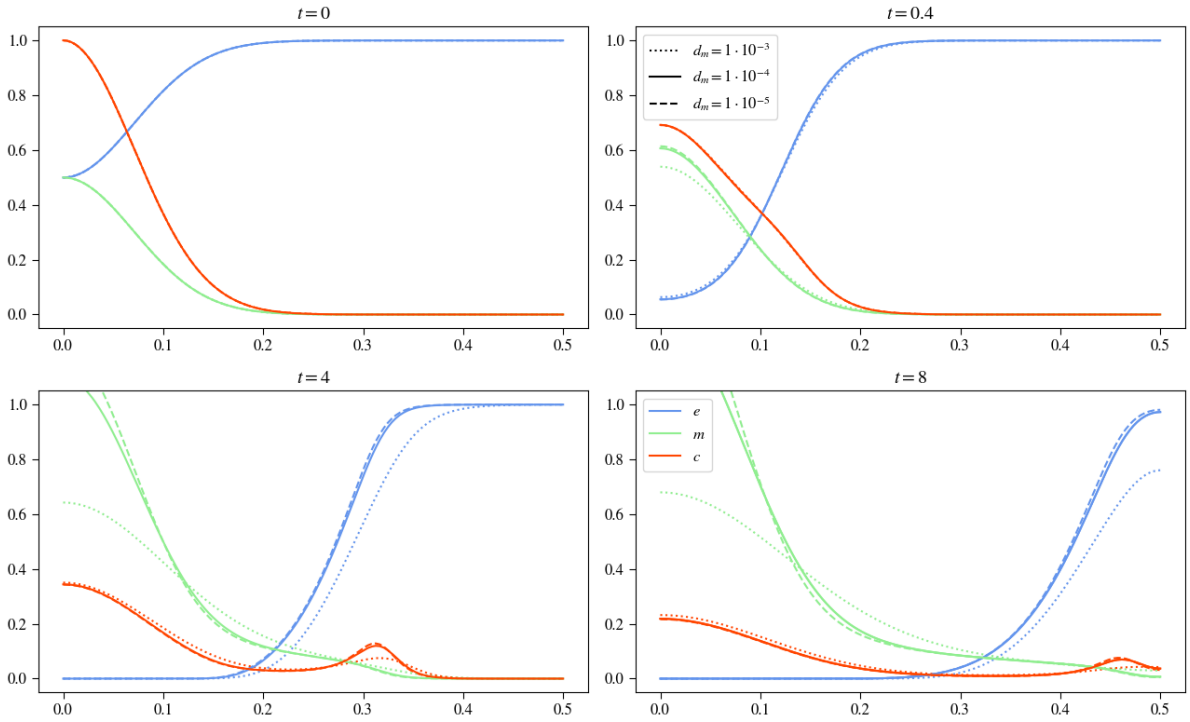

FIGURE 14. Plots show results for varying d_m whilst keeping the other parameters constant, in the images you can see the effects of $d_m = 0.1$ in the dashed curve, $d_m = 0$ in the dotted curve and $d_m = 1 \cdot 10^{-3}$ in the solid line.

higher than for the others the degradation happens more evenly moving outward in the unit square. This pregnant change in the ECM concentration shows also in the tumour cell density. The more even degradation of the ECM makes the haptotaxis effects smaller since ∇e diminishes. As we see the other two curves of the tumour cells developing the secession to form a secondary lump of tumourous cells, we can't see this behaviour here. For the lower two values we see that as expected higher diffusion causes an more even spread of the matrix-degrading enzymes in space and therefore a lower concentration to stay at the origin. Between those two the effects this has on the ECM degradation and the invasion of the tumour cells are only minor.
In the next point in time we see that the constant distribution of MDEs in space, causes an a lot faster degradation process of the ECM, in the previous point in time, the total are of the ECM was still larger, here it is visibly lower than for the lower d_c experiments result's. The tumour cells have only slighlty further invaded the tissue though have a more evenly distribution in space. For the MDE concentration we seee that it has visibly rise to a value of approximately 0.1 everywhere in space. Considering the results of the other two experiments at this point in time, we can observe that a very slow diffusion of the matrix-degrading enzymes causes haptotatic effects to increase. This can be explained with the ECM curves, with the one for the lowest d_m experiment is the most steep one, causing high values for ∇e and therefore a higher haptotaxis value. Interesting to note is that though the ECM degradation happens slowest for the lowest value of d_m the

difference between this and the experiment with a value of $d_m = 0.00001$ in regard to ECM degradation and tumour cell density vary only slightly, considering a difference of two potentces. Also the difference of the tumour cell density at the origin is for the lower two d_m experiments also only minor, though the MDE concentration here has enormous changes, with the experiment for d_m exceeding one by far, and having a total area that is also far larger.
The last point in time shows that the high d_m value has caused the ECM to have degraded completly, and has with this eliminated the effects of haptotaxis on the tumour cells, to have them only subject to diffusion. Looking at the other two experiments we observe the same as for the point in time before, lower d_m values result in a less evenly ECM degradation and a considerably higher MDE concentration at the center, which strongly decreases with distance to it. The effects this has on the tumour cells are only minimal, with a higher influence of haptotaxis for lower d_m values.
Though the differences in the MDE concentration of the lower two d_m experiments are pregnant, the other two curves look roughly the same, while the results with the highest d_m value strongly differ from those. We can conclude that the higher the value of d_m is the more sensitive the system reacts.

α Variation

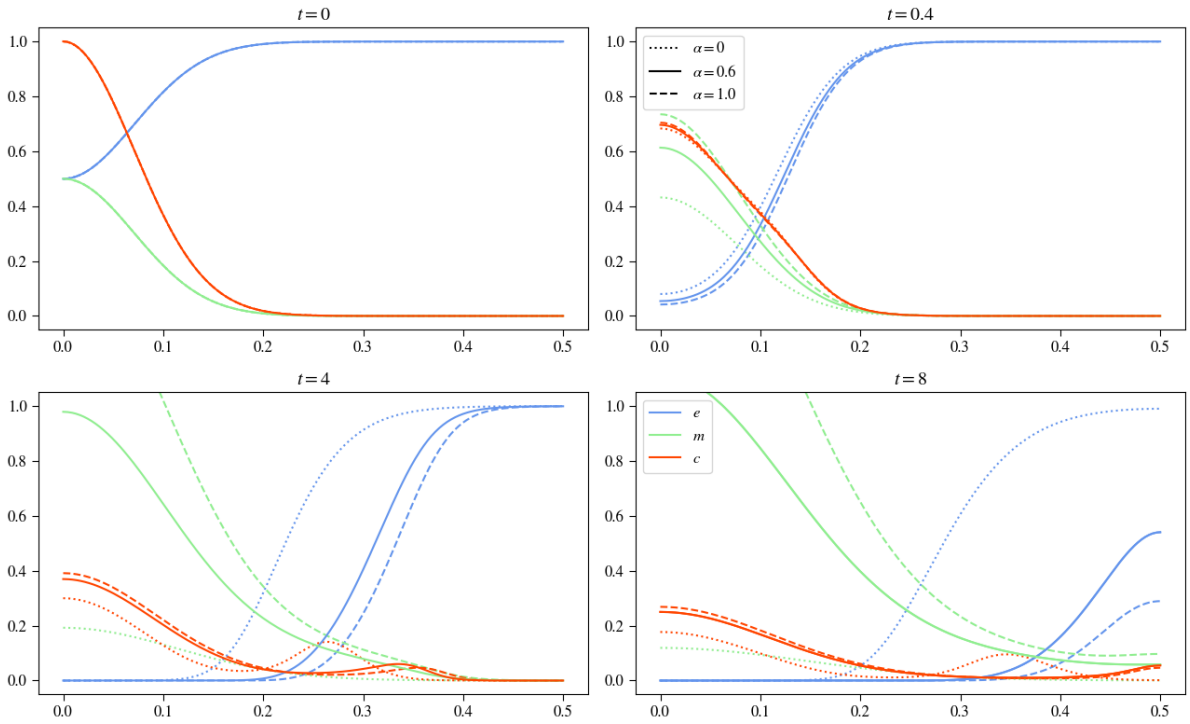

FIGURE 15. Plots show results for varying α whilst keeping the other parameters constant, in the images you can see the effects of $\alpha = 1.0$ in the dashed curve, $\alpha = 0$ in the dotted curve and $\alpha = 0.6$ in the solid line.

The parameter α influences how fast the tumour cells produce matrix decaying enzymes, we assume it to be evenly distributed with $\alpha \sim U[0, 1.0]$. Trying to replicate Anderson et al's experiment we already see how varying α affects the simulation results. With growing α we will see a higher concentration of MDEs especially at the origin. More available MDEs will cause a faster degradation of the ECM first due to having more of them, but also because since more of them are subject to diffusion they will spread faster in the tissue. Faster ECM degrading could mean increased invasion pace of the tumour cells. As we saw in the previous experiments varying d_c, the MDE concentration can take on values higher than one, we can also expect this here when α is sufficiently high.
In the second image of figure 15 describes the experiments after $t = 0.4$. We can see that the difference in the MDE curve for the different values of α is already clearly visible, the higher α the higher the concentration of the MDEs. The other curves seem not be affected as strong at this point in time though we can already see differences for th ECM concentration, with a rising degradation pace as α rises. The curve of the tumour cells looks almost identical for all values of α, looking very closely we can see small deviations around $x = 0$, higher values for α correspond with higher values for the tumour cell density directly at $x = 0$, moving further out, as better seen in later points in time, the amount of cells decreases with rising alpha as haptotatic pull is not as strong in this experiment, due to slowed ECM degradation.
The next point in time at $t = 4$, shows the previous mentioned effects in an intensified way. Whilst for $\alpha = 0$, the dotted curves, the MDEs have no producing factor and the curve flattens due to diffusion. For the ECM we see that though it has degraded visibly this happened at a slower rate than for the other experiments. The tumour cells have lowest density at the origin of the three experiments, but it's hill at the leading edge has the highest volume, as explained above, due to slowed degradataion the tumour cells at the origin are exposed to higher influences of haptotaxis pulling more of the cells into the surrounding tissue. The solid curves describing $\alpha = 0.6$ show that at this point in time they have almost reached a concentration of one at the center, which will be exceeded at the later time steps. With the tumour cells have invaded farther out than in the experiment with the lowest alpha value the ECM degradataion has also been accellerated. Looking at the dotted lined experiment, $\alpha = 1.0$, the value of the MDEs at the origin has already exceeded one by far, with a value of $1,55$ at $x = 0$, thus the degradation is happening faster, with a decreased ECM curve and faster invading tumour cells.
In the last timestep we see that the MDE curve of both $\alpha = 0.6$ and $\alpha = 1.0$ have exceeded one. The dotted curve of the MDE shows that diffusion has distributed the MDE more evenly throughout space, without changing its overall volume. At the border regions we see that the dotted curve is also the only one that has not yet degraded any ECM in this regions, whilst the dashed curve shows that there is only a little ECM concentration left to degrade for the experiment with the highest α value. This is also shown in the curve of the tumour cells, whilst the dotted curve's peak is still somewhere around $x = 0.35$ the other two curves indicate complete invasion of space.
Our initial assumptions are correct with a faster degradation pace due to higher MDE concentration and therefore a faster invasion pace of the tumour cells. Whilst it makes from a numerical perspective sense that the concentration of MDEs can exceed one, it

might make sense to introduce a finer grid or adapt the model in other ways, since judging from a continuous perspective it does not really make sense that at a certain point in space there are more than one entities, occupying this space.

β Variation

The variaton of the decay of the matrix-degrading enzymes β is shown in figure 16. Using Kolev et al's estimate for β in [11] we started experimenting with $\beta = 0.07$. We therefore settled for an even distribution of β in $\beta \sim U[0.005, 0.1]$. Interestingly α and β are, as the experiments will confirm, not of the same magnitude, this is caused by the tumour cells having a constant volume in time and the matrix-degrading enzymes to increase over time. We can assume that with varying β the MDE curve will be lower, influcencing the ECM degrading process and therefore also the invasion pace.

As we see from the results in figure 16 a value of $\beta = 0.1$ is sufficient to after already

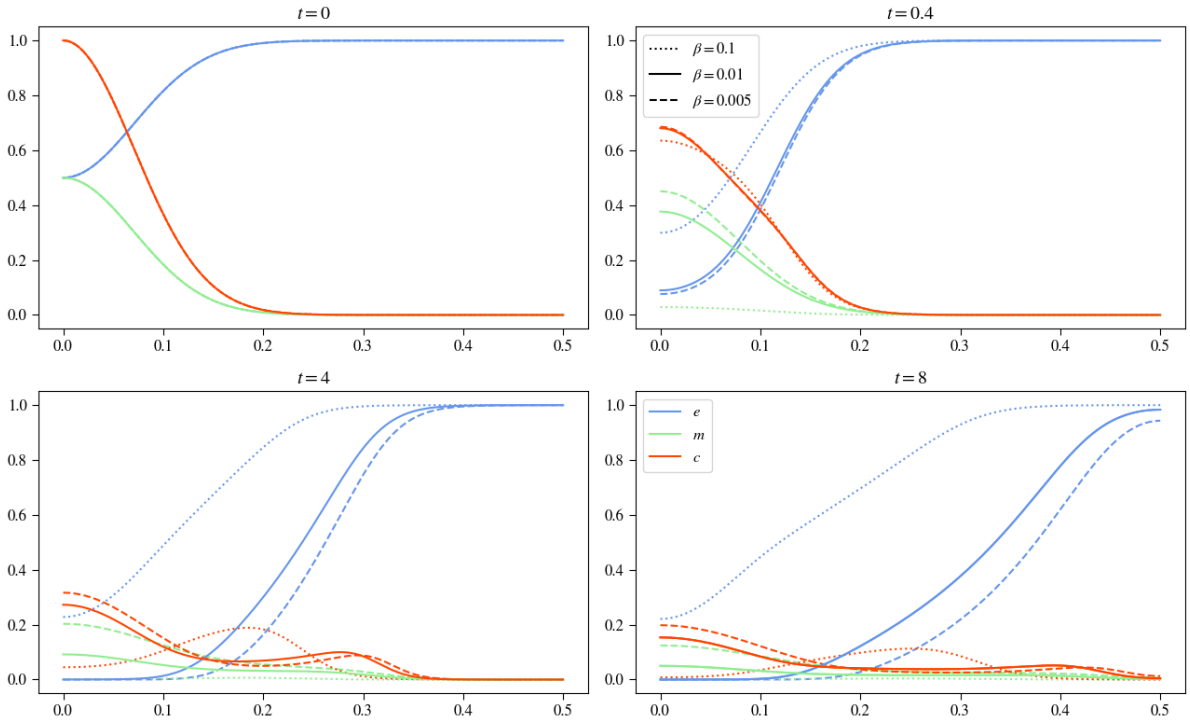

FIGURE 16. Plots show results for varying β whilst keeping the other parameters constant, in the images you can see the effects of $\beta = 0.005$ in the dashed curve, $\beta = 0.1$ in the dotted curve and $\beta = 0.01$ in the solid line.

four timesteps reduce the MDE concentration to zero everywhere. In later points in time this decay rate proves to be too high with a curve of MDE concentration everywhere vanishing spacially and temporaly. The immediate decay of the MDEs causes a slower ECM degradation, yet it has no stopped completely since the tumour cells still produce matrix-degrading enzymes. This slow degradation of extracellular matrix causes the tumour cells to remain as one lump of cells, that moves with its maxima in space, below where ∇e is

highest. We saw this effect previously at the variation of η where the haptotatic pull of the ECM was kept high at the regions near the center, which also caused to stay as only one lump of cells, with the slow ECM degradation we have the same effect here, though here ECM is still degraded at all.
In the other experiments we can observe that with decreasing β and therefore slowing down the decay of the matrix-degrading enzymes, first the ECM degradation accellerates and this causes the effects of haptotaxis and diffusion to develop the two main lumps of tumour cells, one staying at the center the other invading the tissue. Across all experiments we can say that the ECM degradation happens more evenly with rising β.

Cross Variation

Having done all those experiments it will be interesting to see how varying multiple parameters affects the outcome of the simulation. For this we took a look at both supporting and countering effects of variation.

$d_c - \gamma$ Variation

Having set $d_c = 0.00005$ and $\gamma = 0.001$ we see no secession of the tumour cells, the effects of haptotaxis are too small leaving the tumour cells only subject to diffusion which results in an even distribution process over time, which also causes a slower invasion pace. Because the tumour cells stay in a lump with its maxima at the origin $x = 0$ the MDEs also take on their maximum there, moving farther out they also distribute very evenly. This staying with values around the origin of the MDEs causes a slower ECM degradation. Increasing $\gamma = 0.01$ we see that the effects of haptotaxis are now pregnantly visible with a very sharp maxima seen at $t = 4$, which equals the maxima of the remaining tumour cell lump at $x = 0$. Stronger influence of haptotaxis leads to a faster invasion pace of the tumour cells into the tissue and allowing to create matrix-degrading enzymes in their wake, causing a more even distribution compared to $\gamma = 0.001$ and also a faster ECM degrading process. Looking at the right side of the plot 17 we see the results for $d_c = 0.1$ here for both γ values diffusion overshadows the effects of haptotaxis completely, with after already $t = 0.4$ having a constant distribution of tumour cells throughout space. Due to this fast spread of tumour cells, the MDEs are also produced evenly throughout space, and an even faster ECM degradataion.

$d_m - \eta$ Variation

Looking at low values for both d_m and η in the figure 18, the dotted curve in the left column, we see that slow diffusion of the matrix-degrading enzymes and slow degradation of the extracellular matrix causes the tumour cells to only develop one lump that invades space, due to stronger haptotatic exposition to a slower degraded ECM, to create larger values for $\nabla(c\nabla e)$, this is also observable for the higher diffusion values and lowwer ECM degrading factors. Having this single lump with a lower maxima and larger length causes the MDEs to produce more evenly farther away from the origin. The low value for the ECM degrading factor results in an overall slower ECM degradation. Looking on the solid

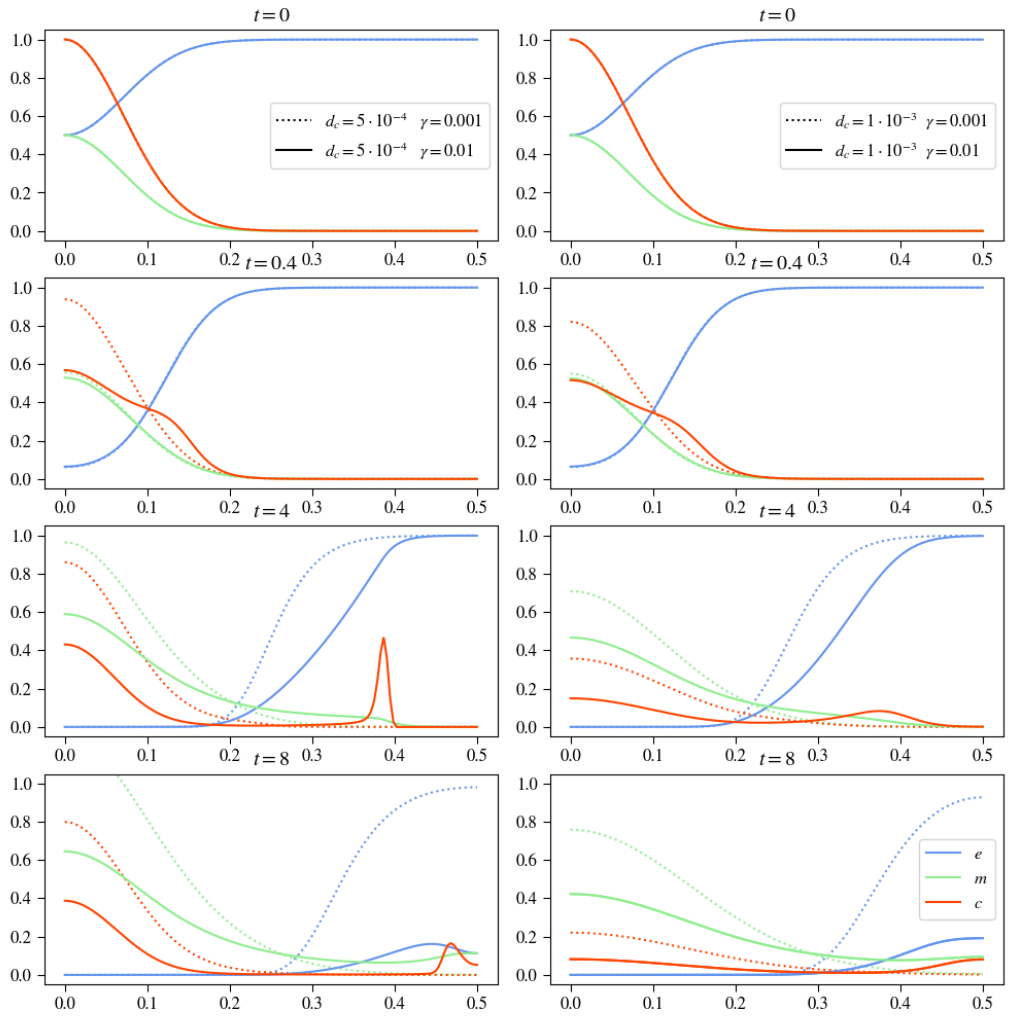

FIGURE 17. Plots show results for varying both d_c and γ whilst keeping the other parameters constant, in the images on the left d_c is set to $d_c = 0.00005$ with the solid line showing $\gamma = 0.01$ and the dotted line $\gamma = 0.001$ on the right d_c is set to $d_c = 0.1$ with the solid line showing $\gamma = 0.01$ and the dotted line $\gamma = 0.001$.

line on the left colum we see that increasing η enables the tumour cells to develop two hills, one staying at $x = 0$ and one invading space by haptotatic pull. Due to a higher density of tumour cells at the origin the MDEs produced there exceed a value of one and ECM degrading happens faster due to first the higher coefficient but also because of a faster invasion pace of matrix-degrading enzymes, due to faster invasion of the tumour cells. Increasing d_m to $d_m = 0.1$ causes the MDE concentration to flatten throughout space, taking on a constant distribution in space for one point in time, neglecting the values for η. Though η still has an influence on both tumour cell density and ECM concentration. We see that, as previously mentioned, for $\eta = 2$ the degrading happens so slow that the tumour cells form only one lump invading the tissue, with its maxima travelling along the x-axis. In contrast to this for $\eta = 20$, we also see only one lump develop though this one stays with it's maxima at the origin. For $\eta = 20$ we see that after $t = 4$ the ECM

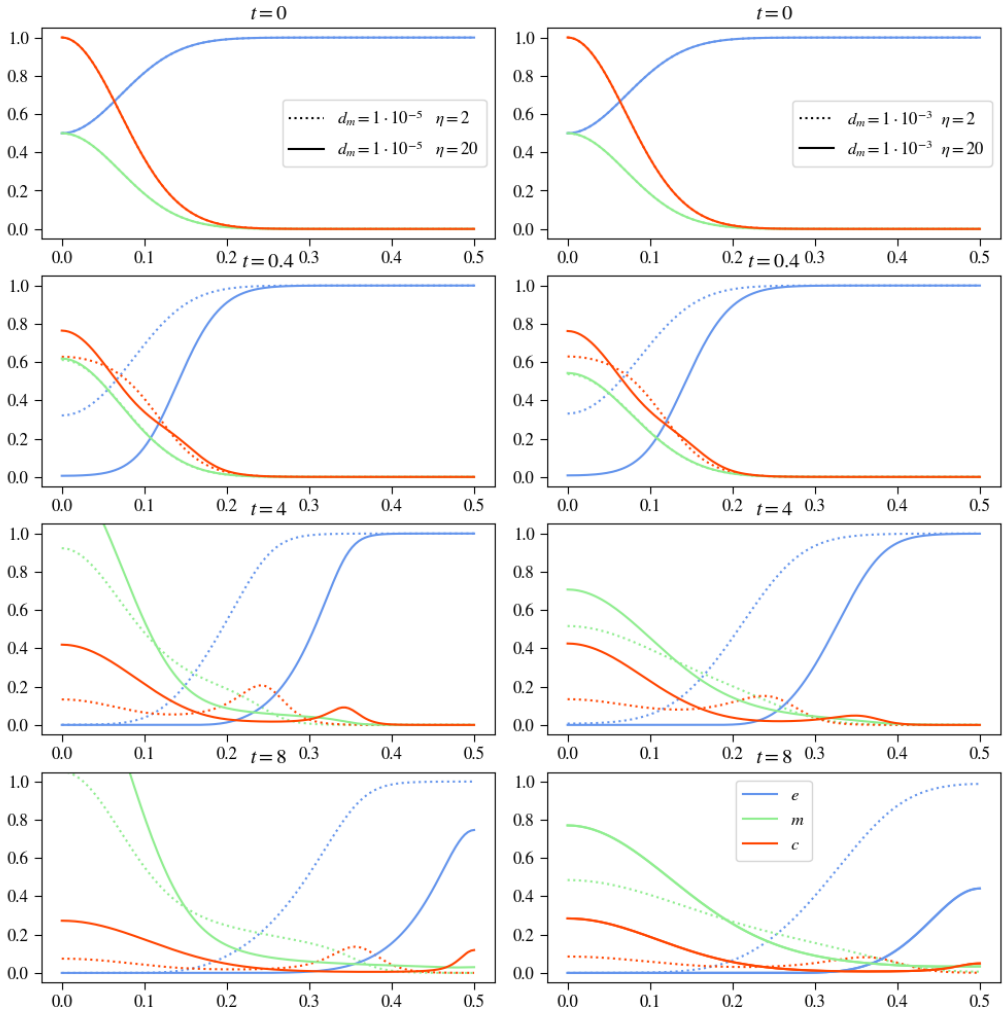

FIGURE 18. Plots show results for varying both d_m and η whilst keeping the other parameters constant, in the images on the left d_m is set to $d_m = 0.0000000001$ with the solid line showing $\eta = 2$ and the dotted line $\eta = 20$ on the right d_m is set to $d_m = 0.1$ with the solid line showing $\eta = 2$ and the dotted line $\eta = 20$.

has almost completly degraded, making the formation of a secondary lump invading the tissue not possible due to too low haptotatic pull.

$\alpha - \beta$ Variation

Looking at figure 19 we see experimental results varying both α and β. For low MDE production but also low MDE decay we can see that the curve for the MDEs is still visible at up to $t = 4$, at $t = 8$ it is zero. We see that first the ECM degrading happens faster than for high β values and therefore the tumour cells develop two lumps with one invading the tissue the other staying at $x = 0$. The maxima for both lumps is lower than in previous experiments, though the cells seem to be more evenly distributed in between the two lumps. Increasing $\beta = 0.1$ the MDE curve seems to be zero after already $t =$ and stays there until the end of this experiment. This low concentration of MDEs casuses a slower

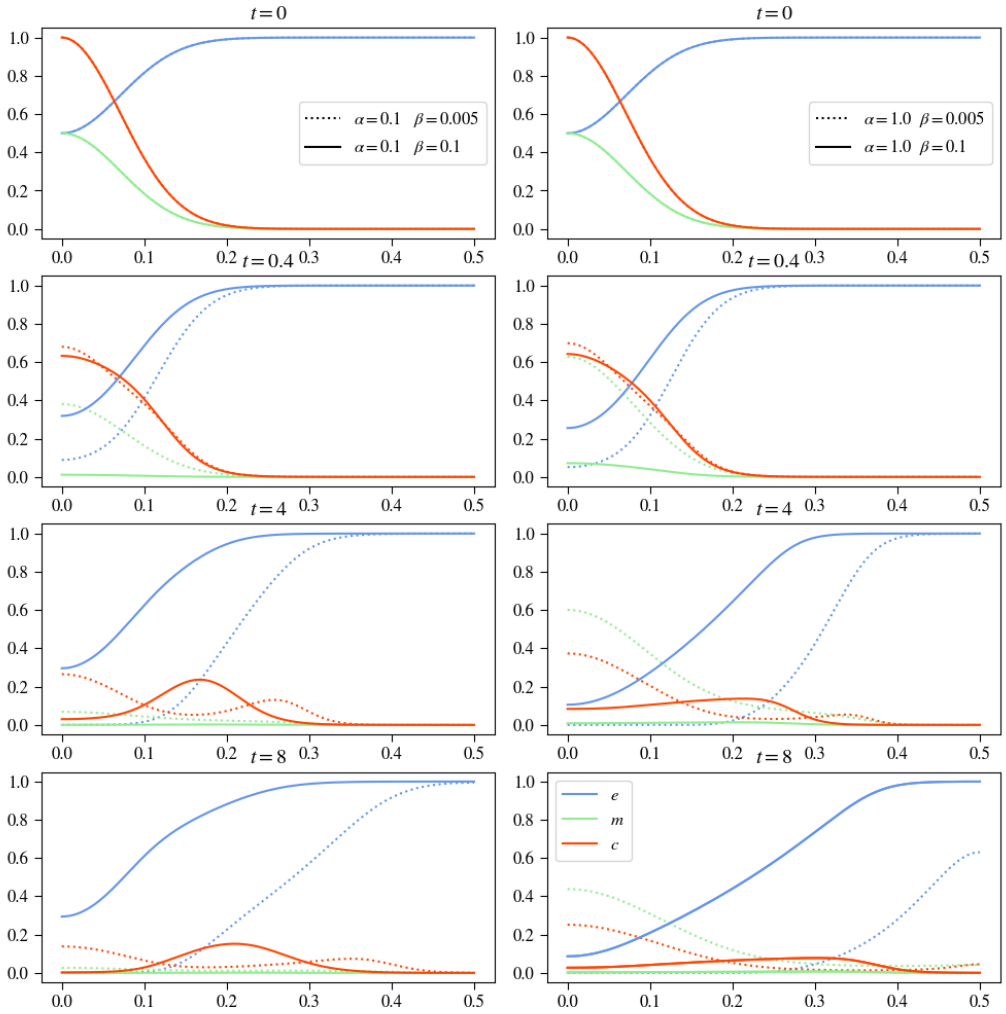

FIGURE 19. Plots show results for varying both α and β whilst keeping the other parameters constant, in the images on the left $\alpha = 0.1$ with the solid line showing $\beta = 0.005$ and the dotted line $\beta = 0.1$ on the right $\alpha = 1.0$ with the solid line showing $\beta = 0.005$ and the dotted line $\beta = 0.1$.

ECM degrading process and therefore leads the tumour cells to only develop one lump, invading the space, with its maxima moving at the center of this lump. For $\alpha = 0.1$ both values for β have proven to be to high, decaying the matrix-degrading enzymes too fast to keep up with production. On the other hand increasing α to 1.0 and keeping $\beta = 0.05$, we see that production outweighs decay, with at the end of the experiment the MDEs still have a concentration of about 0.4 at $x = 0$. For this experiment we seee that the tumour cells develop two lumps indicating that diffusion and haptotaxis effects are also in some balance, and ECM degradation seems to resemble due to similiarities with the basecase for the MDE curve, also the ECM degradation of the basecase experiment. Increasing both α and β we see in the solid line of the right column of figure 19 that decay outweighs production again, after $t = 0.4$ we can only see a small remaining portion of matrix-degrading enzymes at the origin. This causes a slower ECM degradataion and therefore

to forming only one lump of tumour cells, due to too strong effects of haptotaxis, though this singular lump is streched flat along the x-axis.

$d_m - \alpha - \beta$ Variation

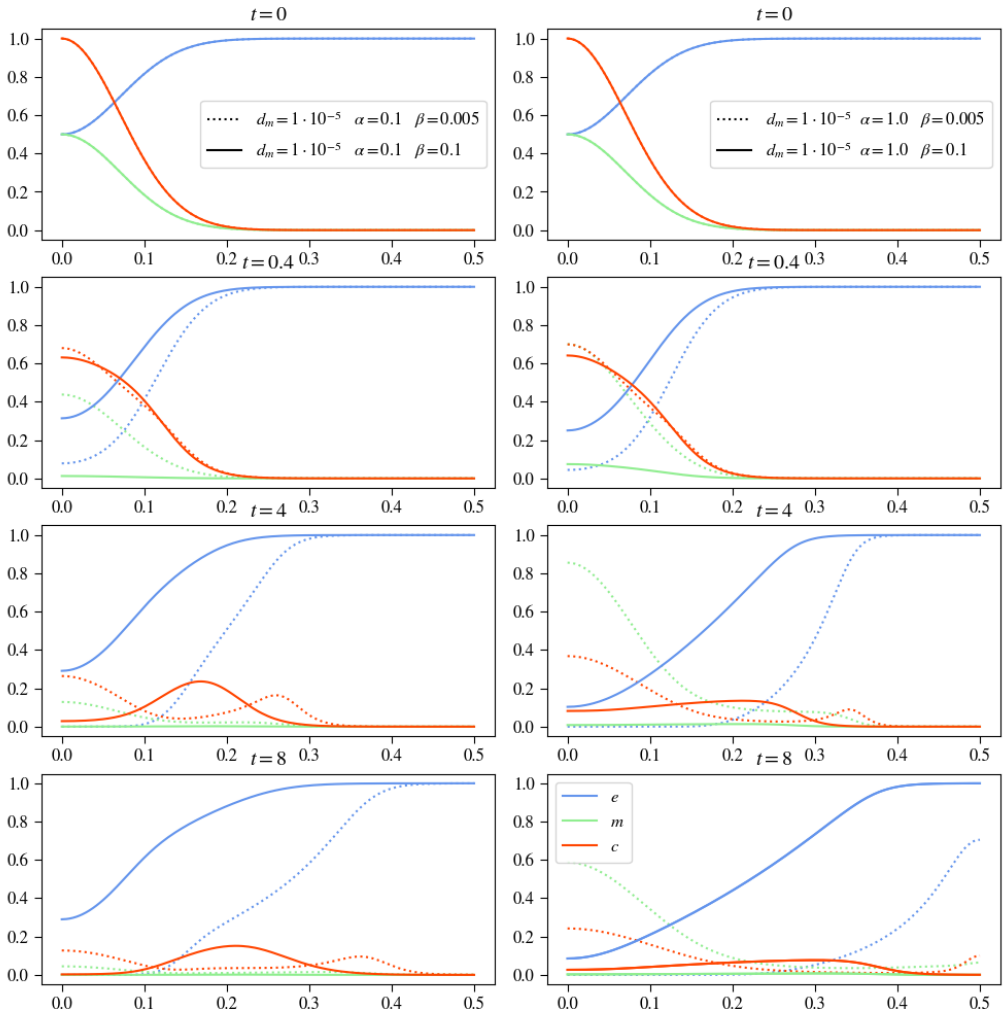

FIGURE 20. Plots show results for varying both α and β whilst keeping the other parameters constant, in the images on the left $\alpha = 0.1$ with the solid line showing $\beta = 0.005$ and the dotted line $\beta = 0.1$ on the right $\alpha = 1.0$ with the solid line showing $\beta = 0.005$ and the dotted line $\beta = 0.1$.

Experimenting with all parameters regarding the equation for the matrix-degrading enzymes required to split the results into two figures, 20 and 21, due to clarity reasons. We are first going to take a look at the results in figure 20, to see the effect of a decreased diffusion coefficient for the MDEs. We observe that with having $\alpha = 0.1$ and $\beta = 0.005$ the ECM degradation happens faster due to having a higher MDE concentration, because of lower MDE decay. Which also increases the seperation of the effects of haptotaxis and diffusion on the tumour cells, seperating them into two lumps, one being pulled them

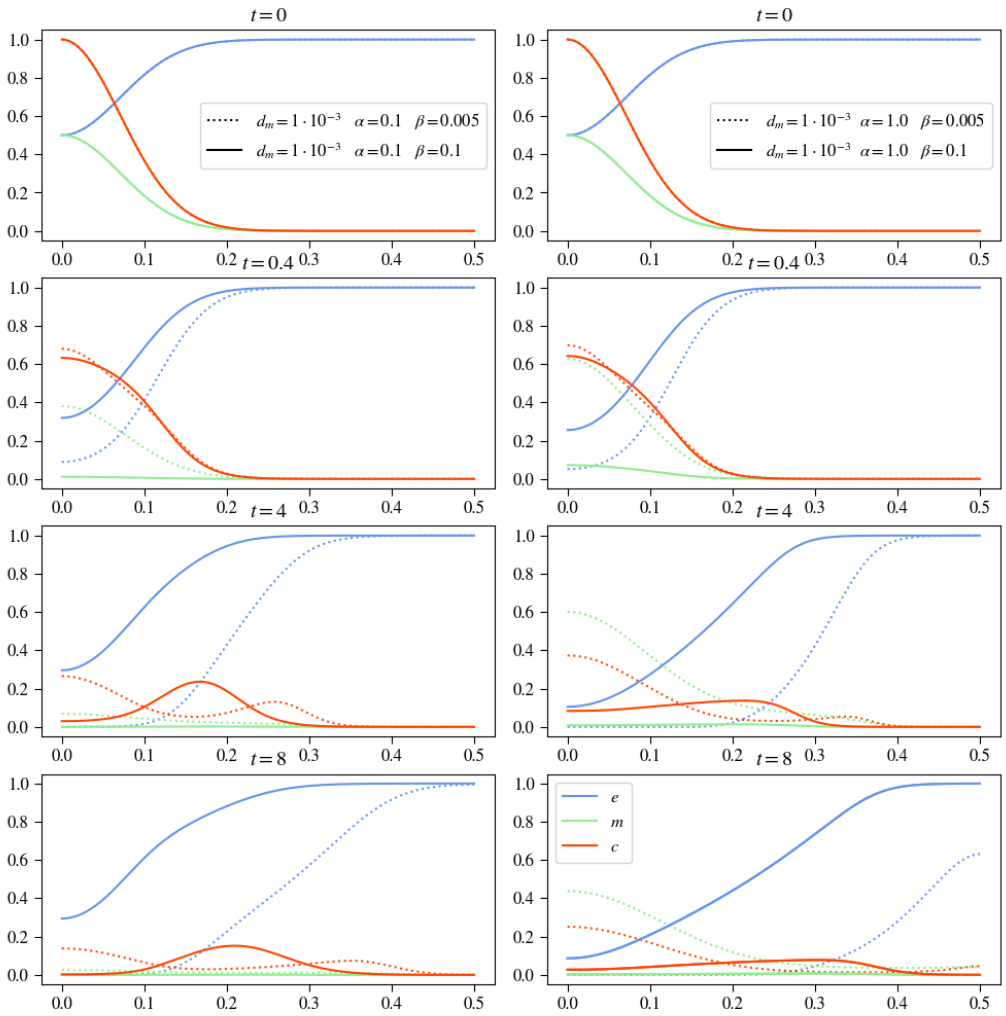

FIGURE 21. Plots show results for varying both α and β whilst keeping the other parameters constant, in the images on the left $\alpha = 0.1$ with the solid line showing $\beta = 0.005$ and the dotted line $\beta = 0.1$ on the right $\alpha = 1.0$ with the solid line showing $\beta = 0.005$ and the dotted line $\beta = 0.1$.

along the ECM faster into the tissue the other staying at the origin. Though the MDE concentration diminishes over time we can still see little remaining concentration at the end at $t = 8$. Increasing β diminishes the MDE concentration sharply, slowing down the ECM degrading process, which increases the effect of haptotaxis over diffusion to pull all of the tumour cells away from the origin to invade the tissue as one lump though at a slower pace. Over time we can see that as expected the tumour cell density's maximum is located approximately right below where $\nabla(c\nabla e)$ is highest.
Looking at the experiments with higher α values we can see that for lower β values the MDE concentration oscilates up and down over time, which indicates that with this configuration of α and β values we found a balancing point. For higher β values we cannot observe this balance, since in this case the MDEs have nearly decayed after $t = 4$. Having such differences in the MDE concentration we can also see big differences in the

ECM concentration. Here we see that as expected with $\beta = 0.005$ the ECM degradation happens a lot faster than having $\beta = 0.1$. These changes in the ECM concentration also affect the tumour cell density. Like in the experiments with $\alpha = 0.1$ the results for having higher β lead to only one lump invading the tissue with a more even distributed density along the x-axis, whereas lower β values made the diffusion and haptotaxis differentiable forming two lumps one to stay at the origin, one to invade the tissue outwards.
Next we are investigating how changing d_m as well will affect the system, looking at figure 21. First of all it is to say that as with varying d_m only the diffusion here is also strong enough to in most cases completely evenly distribute the matrix-degrading enzymes in all of the space after already the fourth step in time.
On the left side we see the experiments with low α values and see that less decay of the MDEs leads to slower ECM degradataion. Due to the very even distribution of the MDEs we see for both cases a more evenly degradation of the ECM, with overall lower gradients. This results in a longer exposition of haptotatic effects on the tumour cells to form only lump invading the tissue with a moving maximum, though for a lower β factor we see that a larger is staying at the origin since the haptotatic pull here is weaker due to having also a more evenly distributed tumour cell density.
Looking at the right side of figure 21 we see with increased α the results regarding the tumour cell density differ strongly. Whereas on the left side we saw that there was always one lump to invade the cells with its maximum moving below where $\nabla(c\nabla e)$ is strongest, we see that for low β the lump of tumour cell stays with its core at the origin at $x = 0$, where also its maximum is, and invades the tissue with no leading edge. This shows the effect of a both sufficiently fast and efficient degradation of extracellular matrix. Here we see diffusion as the main factor for the movement of the tumour cells since the haptotatic pull is very low, due to small gradients of e only. For the other curves we can observe that as before with rising β the ECM degradation pace slows down, in the last point in time the difference β causes is pregnantly visible with for low β the ECM has been degraded completely but for high β there is still a considerable concentration. Looking at the MDE concentration we can also see clear differences regarding the influence of the diffusion on the MDE decay. Though the MDE concentration with high diffusion is more evenly distributed, its overall volume in space is clearly lower than for low diffusion terms, with same α and β configuarations.

4.2 Two dimensional Results with Proliferation and Renewal

In this section we are going to inspect the updated system, consisting of equation 6 to 10, to describe the effects of tumour cell proliferation and extracellular matrix renewal processes. Like for the model neglecting proliferation and renewal we can see in table 2 all the experiments done in two space dimensions using the updated model.

Figure	Linestyle	d_c	γ	μ_1	η	μ_2	d_m	α	β
22	.....	$5 \cdot 10^{-4}$	0.0055	0	10	0	$1 \cdot 10^{-3}$	0.3564	0
22	——	$5 \cdot 10^{-4}$	0.0055	0.1	10	0.5	$1 \cdot 10^{-3}$	0.3564	0

continued on next page

Figure	Linestyle	d_c	γ	μ_1	η	μ_2	d_m	α	β
23	·····	0.1	0.0055	0.1	10	0.5	$1 \cdot 10^{-3}$	0.3564	0
23	——	$1 \cdot 10^{-3}$	0.0055	0.1	10	0.5	$1 \cdot 10^{-3}$	0.3564	0
23	- - - -	0.00005	0.0055	0.1	10	0.5	$1 \cdot 10^{-3}$	0.3564	0
24	·····	$5 \cdot 10^{-4}$	0.002	0.1	10	0.5	$1 \cdot 10^{-3}$	0.3564	0
24	——	$5 \cdot 10^{-4}$	0.008	0.1	10	0.5	$1 \cdot 10^{-3}$	0.3564	0
24	- - - -	$5 \cdot 10^{-4}$	0.01	0.1	10	0.5	$1 \cdot 10^{-3}$	0.3564	0
25	·····	$5 \cdot 10^{-4}$	0.0055	0	10	0.5	$1 \cdot 10^{-3}$	0.3564	0
25	——	$5 \cdot 10^{-4}$	0.0055	0.5	10	0.5	$1 \cdot 10^{-3}$	0.3564	0
25	- - - -	$5 \cdot 10^{-4}$	0.0055	1.0	10	0.5	$1 \cdot 10^{-3}$	0.3564	0
26	·····	$5 \cdot 10^{-4}$	0.0055	0.1	0	0.5	$1 \cdot 10^{-3}$	0.3564	0
26	——	$5 \cdot 10^{-4}$	0.0055	0.1	12	0.5	$1 \cdot 10^{-3}$	0.3564	0
26	- - - -	$5 \cdot 10^{-4}$	0.0055	0.1	20	0.5	$1 \cdot 10^{-3}$	0.3564	0
27	·····	$5 \cdot 10^{-4}$	0.0055	0.1	10	0.1	$1 \cdot 10^{-3}$	0.3564	0
27	——	$5 \cdot 10^{-4}$	0.0055	0.1	10	0.6	$1 \cdot 10^{-3}$	0.3564	0
27	- - - -	$5 \cdot 10^{-4}$	0.0055	0.1	10	1.0	$1 \cdot 10^{-3}$	0.3564	0
28	·····	$5 \cdot 10^{-4}$	0.0055	0.1	10	0.5	0.00001	0.3564	0
28	——	$5 \cdot 10^{-4}$	0.0055	0.1	10	0.5	$1 \cdot 10^{-3}$	0.3564	0
28	- - - -	$5 \cdot 10^{-4}$	0.0055	0.1	10	0.5	0.1	0.3564	0
29	·····	$5 \cdot 10^{-4}$	0.0055	0.1	10	0.5	$1 \cdot 10^{-3}$	0	0
29	——	$5 \cdot 10^{-4}$	0.0055	0.1	10	0.5	$1 \cdot 10^{-3}$	0.6	0
29	- - - -	$5 \cdot 10^{-4}$	0.0055	0.1	10	0.5	$1 \cdot 10^{-3}$	1.0	0
30	·····	$5 \cdot 10^{-4}$	0.0055	0.1	10	0.5	$1 \cdot 10^{-3}$	0.3564	0.1
30	——	$5 \cdot 10^{-4}$	0.0055	0.1	10	0.5	$1 \cdot 10^{-3}$	0.3564	0.01
30	- - - -	$5 \cdot 10^{-4}$	0.0055	0.1	10	0.5	$1 \cdot 10^{-3}$	0.3564	0.005
31 - left	·····	$5 \cdot 10^{-4}$	0.0055	0.1	10	0.1	$1 \cdot 10^{-3}$	0.3564	0
31 - left	——	$5 \cdot 10^{-4}$	0.0055	0.1	10	1.0	$1 \cdot 10^{-3}$	0.3564	0
31 - right	·····	$5 \cdot 10^{-4}$	0.0055	1.0	10	0.1	$1 \cdot 10^{-3}$	0.3564	0
31 - right	——	$5 \cdot 10^{-4}$	0.0055	1.0	10	1.0	$1 \cdot 10^{-3}$	0.3564	0
32 - left	·····	0.00005	0.001	0.1	10	0.5	$1 \cdot 10^{-3}$	0.3564	0
32 - left	——	0.00005	0.001	1.0	10	0.5	$1 \cdot 10^{-3}$	0.3564	0
32 - right	·····	0.00005	0.01	0.1	10	0.5	$1 \cdot 10^{-3}$	0.3564	0
32 - right	——	0.00005	0.01	1.0	10	0.5	$1 \cdot 10^{-3}$	0.3564	0
33 - left	·····	0.1	0.001	0.1	10	0.5	$1 \cdot 10^{-3}$	0.3564	0
33 - left	——	0.1	0.001	1.0	10	0.5	$1 \cdot 10^{-3}$	0.3564	0
33 - right	·····	0.1	0.01	0.1	10	0.5	$1 \cdot 10^{-3}$	0.3564	0
33 - right	——	0.1	0.01	1.0	10	0.5	$1 \cdot 10^{-3}$	0.3564	0
34 - left	·····	$5 \cdot 10^{-4}$	0.0055	0.1	2	0.1	$1 \cdot 10^{-3}$	0.3564	0
34 - left	——	$5 \cdot 10^{-4}$	0.0055	0.1	2	1.0	$1 \cdot 10^{-3}$	0.3564	0
34 - right	·····	$5 \cdot 10^{-4}$	0.0055	0.1	20	0.1	$1 \cdot 10^{-3}$	0.3564	0
34 - right	——	$5 \cdot 10^{-4}$	0.0055	0.1	20	1.0	$1 \cdot 10^{-3}$	0.3564	0

continued on next page

Figure	Linestyle	d_c	γ	μ_1	η	μ_2	d_m	α	β

TABLE 2. Overview of all experiments conducted for the model with proliferation and renewal producing 2D output

Basecase Analysis

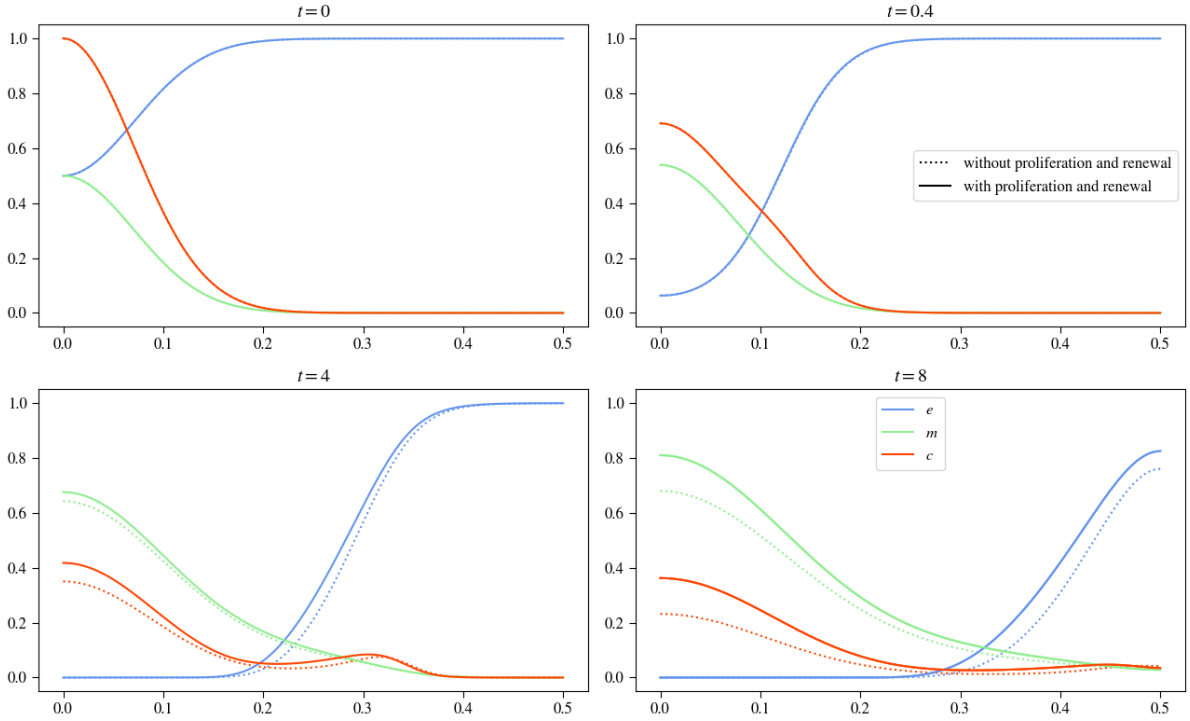

FIGURE 22. Describing the updated basecase, in the image above only the updated basecase is plotted, below it is compared to the initial basecase.

Here is also makes sense to establish a basecase to compare the following parameter analysis resulst against. In figure 22 you can see how intoducting tumour cell proliferation and extracellular matrix renewal changes the outcome of the simulation. For this we used the values $\mu_1 = 0.1$ and $\mu_2 = 0.5$ according to the only experiment found for this system of equations in the paper of Kolev et al. [11].
Comparing this new basecase to our initial model's basecase we can see the influences of both μ_1 and μ_2, as for the tumour cell density curve is visibly higher than without proliferation, causing a higher production of matrix-degrading enzymes, which would lead to faster ECM degradation, though this is countered by the renewal factor μ_2 causing the ECM concentration to be higher at the end, at $t = 8$, than in the initial basecase experiment.

4.2.1 Parameter Analysis

For the Parameter Analysis of the model with proliferation and renewal we are focusing on comparing the results of the updated model with the results produced by the model without renewal and proliferation, this will point out again the influence of μ_1 and μ_2 on the system.

d_c Variation

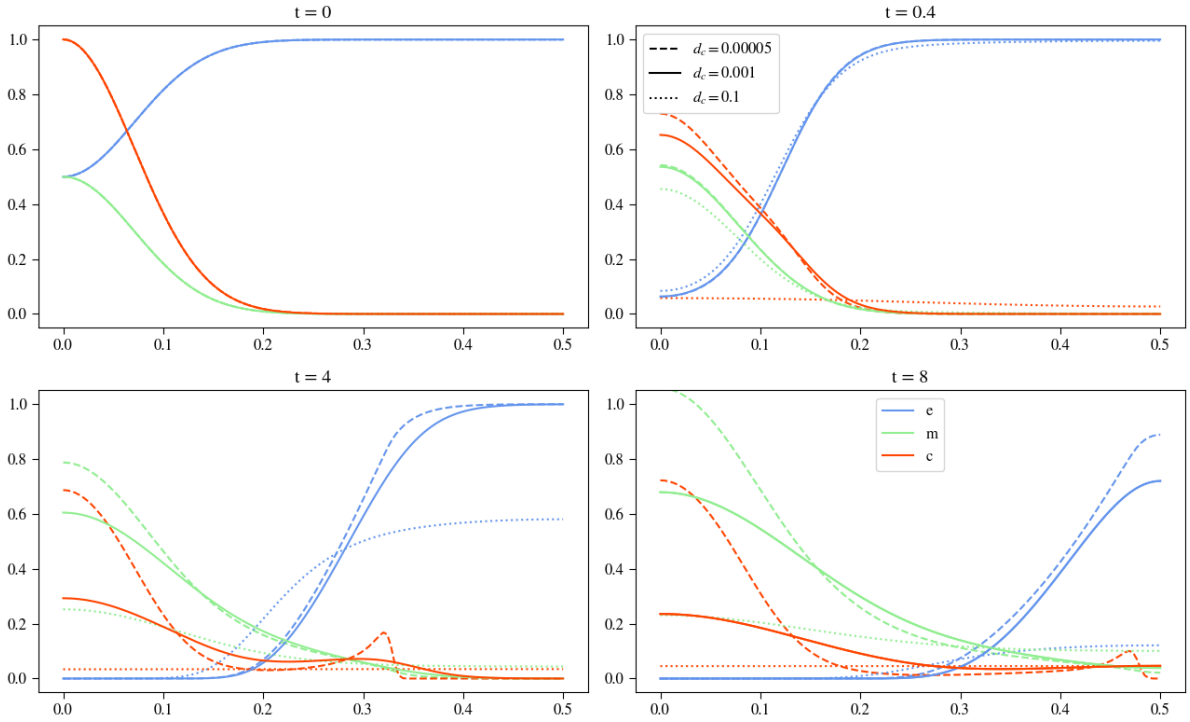

FIGURE 23. Plots show results for varying d_c whilst keeping the other parameters constant

Varying d_c with proliferation terms, we see the same effects as without proliferation. Higher values for d_c cause a stronger influence of diffusion and a weaker for the haptotaxis, which leads to a curve with less or none of a leading edge invading the space, but to a faster rather constant distribution throughout space. The MDE concentration follows this behaviour, depending on its production on the tumour cell density distribution in space and the ECM is decayed faster, the faster the tissue is invaded, thus the higher the diffusion factor is. Comparing them we see little differences, only tumour cell density and ECM are raised a little in each plot due to the renewal and proliferation factors, which in turn also causes a higher MDE concentration, due to higher tumour cell densities.

γ Variation

When we look at γ we also can see the same effects as the model without proliferation shows, with the adjustments as varying d_c, with raised curves for all variables. Increasing

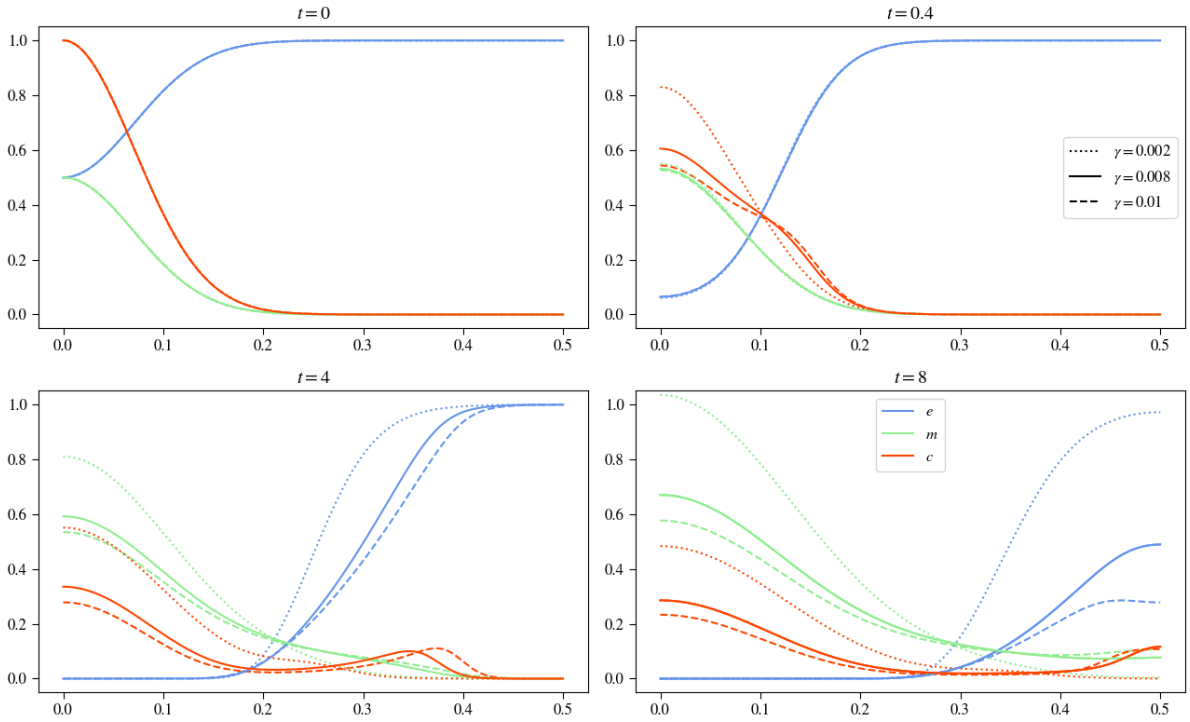

FIGURE 24. Plots show results for varying γ whilst keeping the other parameters constant.

γ means increasing haptotaxis effects, pulling the tumour cells stronger towards the extracellular matrix molecules, which causes a faster invasion pace and also a higher density of tumour cells invading the tissue, but a lower staying at the centere at $x = 0$. This also means that the ECM degrading process happens faster and the MDEs are more evenly distributed through space the higher γ is. As mentioned above the same effects come in this experiment, introducing proliferation and renewal, with higher values for tumour cell density, MDE and ECM concentration especially at the later points in time clearly depictable. It is interessting to observe that though introducing a renewal factor for the extracellular matrix, the proliferation of the tumour cells causes a faster production of matrix-degrading enzymes, which makes the system produce nearly the same results as without proliferation and renewal concerning the ECM concentration, still it is to say that introducing the renewal of the ECM results in overall slightly higher concentrations of it.

μ_1 Variation

The parameter μ_1 describes the proliferation of the tumour cells, using Kolev et al's estimate in [11] we can assume an even distribution with $\mu_1 \sim U[0.1, 1.0]$. We see that with varying μ_1 the other curves are also strongly influenced though it takes some time as the plots in figure 25 indicate, with after $t = 0.4$ they seem to overlay each other. At $t = 4$ we see that first of all the tumour cells curve obviously increases with increasing μ_1, this causes the MDE concentration to also increase and in turn the ECM curve is decreased due to faster ECM degradation, because of more availabe matrix-degrading enzumes. At

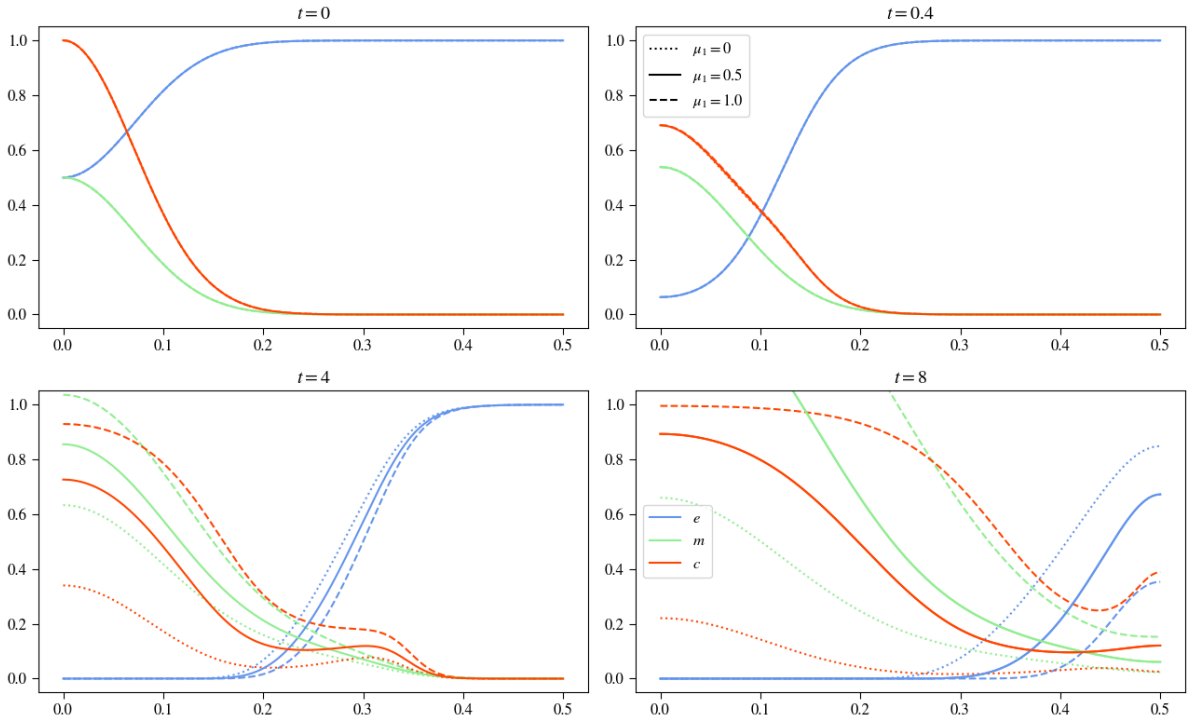

FIGURE 25. Plots show results for varying μ_1 whilst keeping the other parameters constant.

the last point in time this befaviour intensifies, the tumour cells having for high μ_1 values a density of one in the range of x being between 0 and 0.2 and for $\mu_1 = 0.5$ also a lot higher than without proliferation of tumour cells. The MDE concentration exceeds one for the two higher values for μ_1 and the ECM having again degraded faster. Looking at the dotted curve, we can observe what only renewal does to our system and we see clearly, comparing it to the basecase of the model without proliferation, that the concentration of the extracellular matrix especially at the end is visibly higher.

η Variation

As we compare the η variation between with and without proliferation and renewal models we see mostly the same effects. For the solid and dashed curves we see little though the curves of the new model are all slightly raised. Looking at $\eta = 0$ we see some interesting deviations, at the time point $t = 0.4$ the plots still look rather similar, but looking at $t = 4$ we see that the curve of the tumour cells has a more even distribution along the x-axis and also its maximum is visibly lower with value of about 0.2 at $x = 1.4$ instead of 0.25 at $x = 1.3$. This behaviour is due to the renewal of the ECM, where without proliferation this curve stayed constant throughout the experiment, here it can increase, which it does altering the slope of the curve and therefore influecing the haptotatic pull for the tumour cells, additionally to this the other two experiments showed a visible increase of the tumour cell density and the matrix-degrading enzyme concentration, but only a

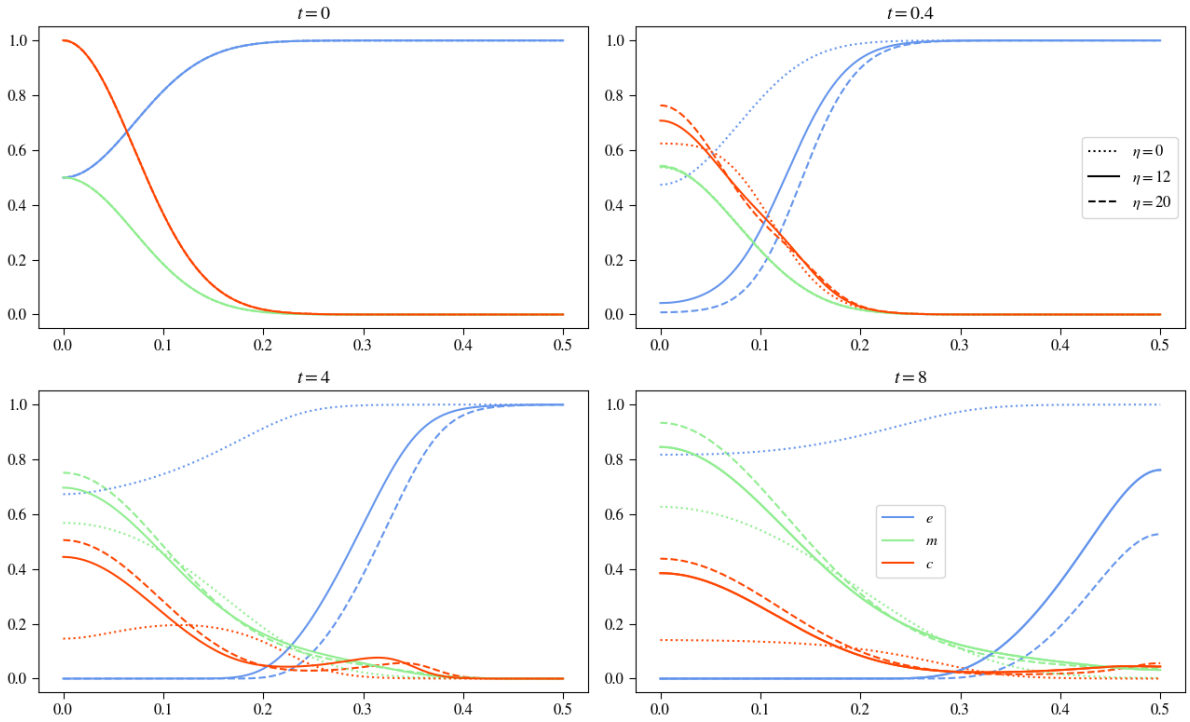

FIGURE 26. Plots show results for varying η whilst keeping the other parameters constant.

slight for the ECM concentration, here we can see no increasing of area for the tumour cell density at all. The renewal of the ECM counters the proliferation of the tumour cells and the slowed ECM degrading process in such a way that at the last two point in time we see that the ECM has visibly increased, with both curves ECM and tumour cells almost mirroring each other. Summing up the areas of both variables we see that they toghether occupy the space completely needed for the logistical growth terms, which means that proliferation and renewal will play no more important role continuing with this experiment as they have reached a equlibrium state and cancel each other out.

μ_2 Variation

The parameter μ_2 describes the renewal processes of the extracellular matrix molecules, with also eusing Kolev et al's estimate in [11] we can assume an even distribution with $\mu_2 \sim U[0.1, 1.0]$.
Like we saw for μ_1 the effects of μ_2 need some time to show, here again we can see them after $t = 4$ timesteps clearly. Wtih higher ECM renewal we see that we get slightly lower MDE maximum at $x = 0$, though having stretched a little more into x-direction. The same goes for the tumour cell density, having a lower maximum at the origin, yet being more evenly distributed, whcih is due to the ECM curve being shifted slightly towards the left, intensifying the effects of haptotaxis. The last image confirms the aforementioned effects with higher ECM concentration due to renewal causes less MDE concentration at its maxima and more stretchig along x-direction, the same holding for the tumour cells.

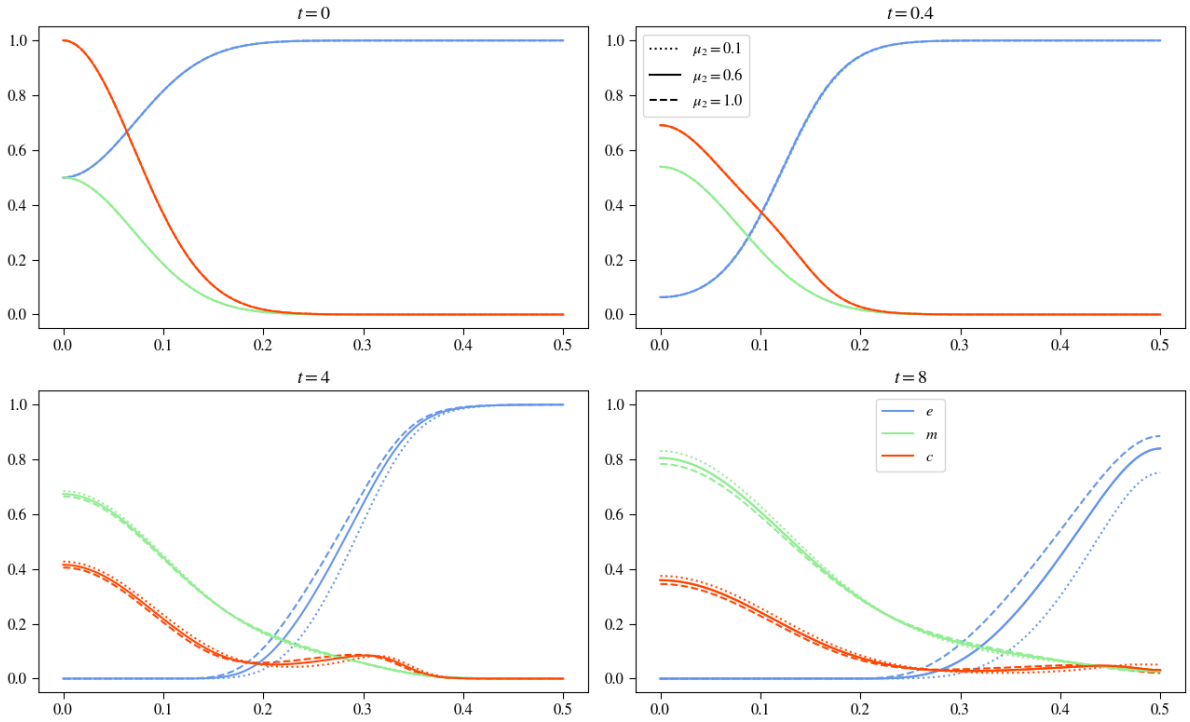

FIGURE 27. Plots show results for varying μ_2 whilst keeping the other parameters constant.

We also observe that the effects of μ_2 are not as impactful on the system as the effects of μ_1 were.

d_m Variation

Comparing the results varying the diffusion factor of the matrix-degrading enzymes does as before yield only minor differences between the initial and updated model. As observed before the tumour cell density's curve and the MDE concentration's curves are slightly raised due to proliferation of the tumour cells. The ECM curve for two lower values of varying d_m though seem to be subject to little to no change, only for very high values of d_m we can see that it is clearly raised comparing it to the model without renewal. The other two curves take off at the some point along the x-axis and finish at the same values for their ECM concentration. Looking at the tumour cell density curves for those d_m values we see that towards $x = 0.5$ they don't describe a as steep bump as the initial model. This causes to have little less MDE concentration as well, which is responsible for the seemingly unchanged behaviour of the extracellular matrix concentration.

α Variation

Taking a look at comparing the α-variation yields more interesting results since, μ_1 acts as a secondary MDE production effect by producing tumour cells which in turn produce the matrix-degrading enzymes. We see that though the overall shape and effects to be

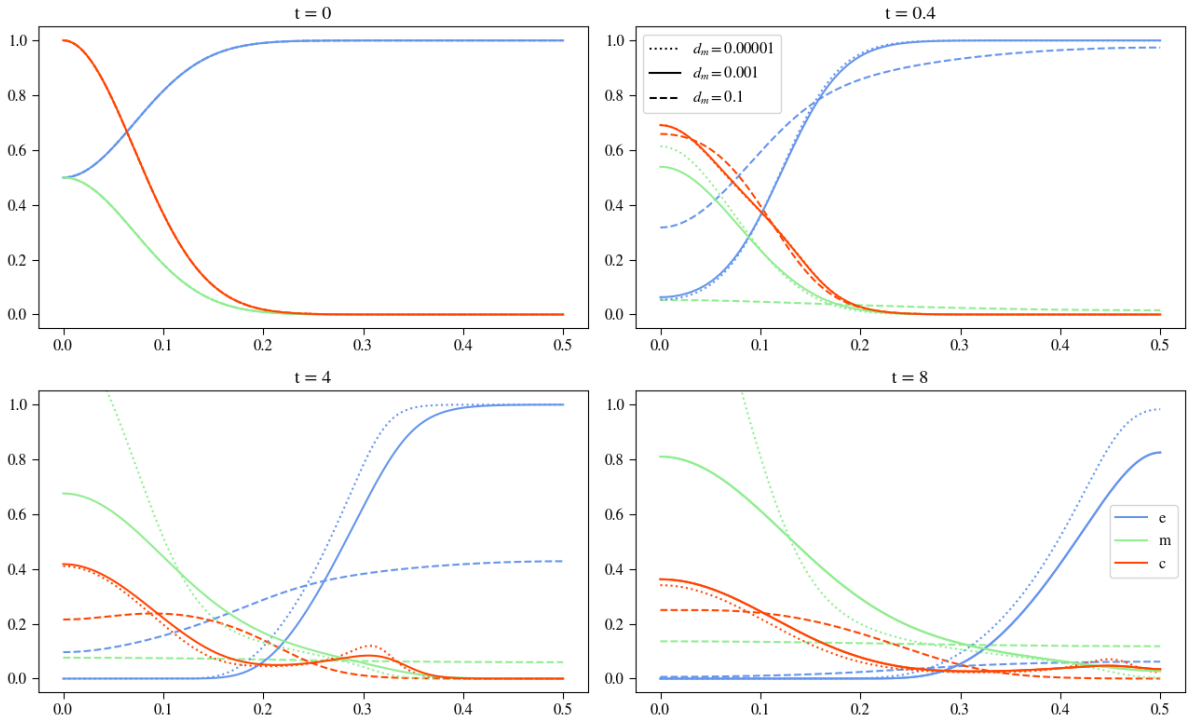

FIGURE 28. Plots show results for varying d_m whilst keeping the other parameters constant.

observed are the same, after $t = 4$ the model with proliferation exceeds one at the origin for the MDE concentration for the two higher α experiments, where in the model without proliferation only the one with the highest α value did. The tumour cell denstiy curve is slightly raised, which allows the MDE concentration. Though the higher values for the MDEs leave the ECM degrading process untouched with not clearly visible difference between the inital model and the updated one.

β Variation

Considering β we can expect that with the introduction of μ_2 the ECM degradation will be slowed considerably with rising β, since this does not only reduce the MDE concentration but does also renew the ECM. Looking at the plots we can see exactly this behaviour in the dotted line, which shows the experiment results for the highest β value of 0.1. Though even at the end it has an overall area that is slightly less than the inital condition we can see going from timestep $t = 0.4$ to $t = 4$ that MDE decay and ECM renewal were sufficiently strong to restore the ECM and going from $t = 4$ to $t = 8$ we see this behaviour again, renewing the ECM. The other two experiments for β showed no effects as strong as with $\beta = 0.1$, yet we can still see the effects of proliferation and renewal especially clear in the solid line, $\beta = 0.01$ at the last point in time, where we can observe a visible increase of both ECM and tumour cell density. In this experiment we see that β is a little too low to counter the effects of ECM degradation, going from $t = 4$ to $t = 8$ we see a

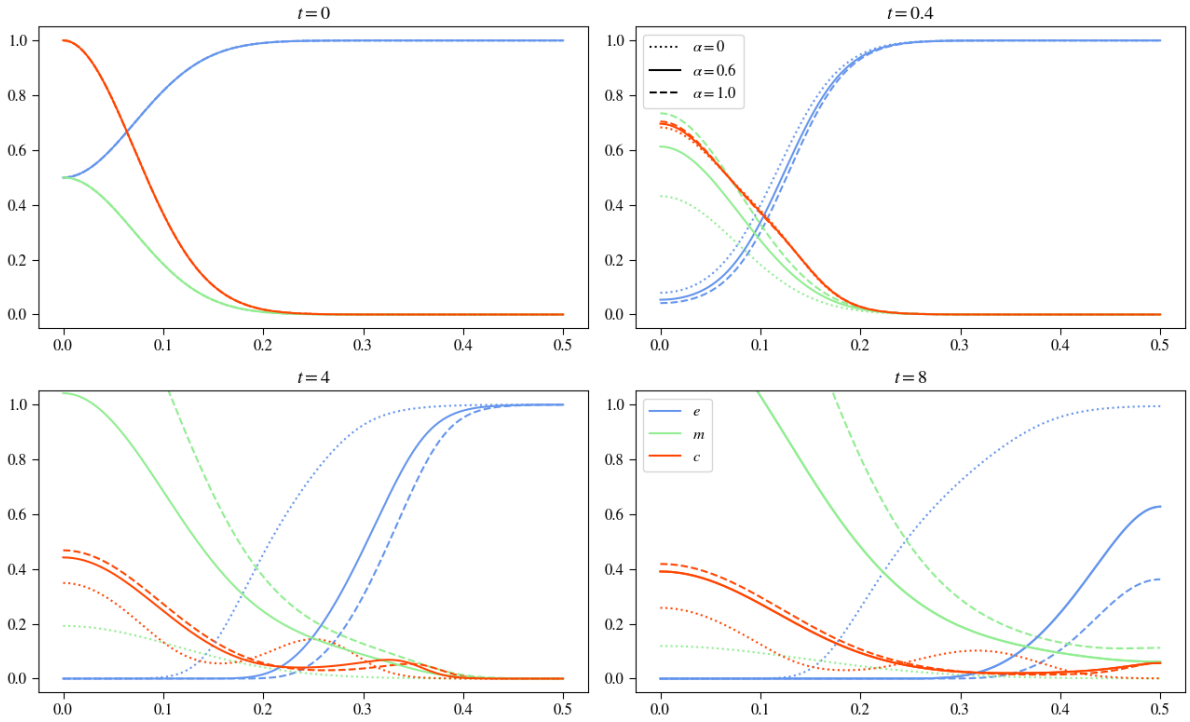

FIGURE 29. Plots show results for varying α whilst keeping the other parameters constant.

clear dicline of ECM concentration though it is not as striking as for $\beta = 0.005$.

Cross Variation

$\mu_1 - \mu_2$ Variation

The effects to observe in this cross variation take some time as did the seperate variations of both μ_1 and μ_2. for both $\mu_1 = \mu_2 = 0.1$ we see that slower ECM renewal and slower tumour ell proliferation increase the degrading process of the extracellular matrix and with this affect the haptotaxis effect to increase slightly. At the center a lump remains that has a maximum a little higher than for the experiment with $\mu_2 = 1.0$ and also the invasion of the tissue has proceeded a little faster. Increasing μ_2, as previously mentioned, results in slower ECM degradation due to the increased renewal term and therefore the tumour cells are stretched out more evenly along the x-axis. Looking at the results when incresing μ_1 we also see the effects only after $t = 4$. For $\mu_2 = 0.1$ we see that the tumour cell density at $x = 0$ is slightly larger as well as at $x \approx 2.9$ the curve for $\mu_2 = 0.1$ is also slightly larger being a little below $\mu_2 = 1.0$ in between $x \approx 0.2$ and $x \approx 0.29$. The curve for the MDEs looks very similar in both cases for μ_2 due to the very similiar tumour cell density curve, c, though th eECM has visibly faster degraded for $\mu_2 = 0.1$ due to the slower renewal.

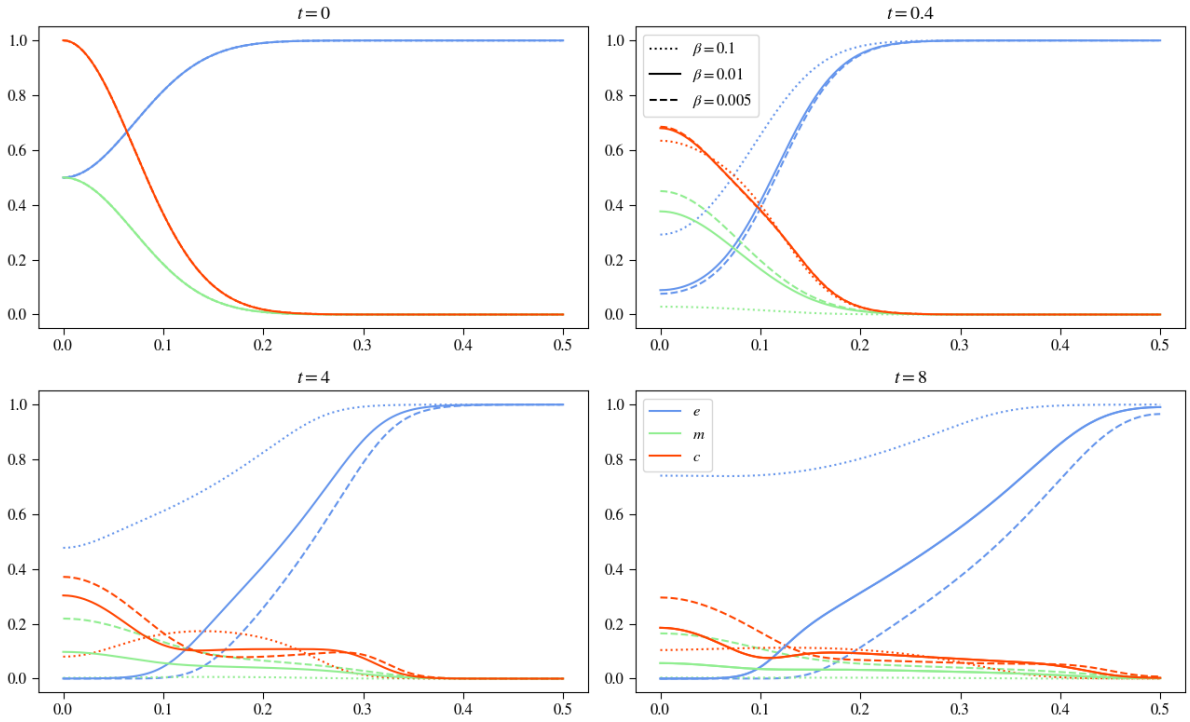

FIGURE 30. Plots show results for varying β whilst keeping the other parameters constant.

$d_c - \gamma - \mu_1$ Variation

First we are goint to take a look at how chaning γ and μ_1 affects the system whils having low diffusion values for the tumour cells with $d_c = 0.00005$, in figure 32. Inspecting the dotted curve on the left side column, shows the results for all parameters set to low, we see that diffusion is tha mian factor for the movement of the tumour cells, with only little influence of haptotaxis, the tumour cells staying with their maximum at the center. Becasue fo this we also get a high MDE concentration there, but very little excedding the region past $x = 0.3$. Due to the MDE also staying centered around thr origin the ECM there is completely degraded, though at $x = 0.4$ and further still completely there. Increasing the proliferation factor to $\mu_1 = 1.0$ shifts the tumour cell density rightwards, making proliferation also a factor for the cell density movement, though keeping the same shape as the low proliferation factor experiment. This right shift causes the MDE concentration to also shift to the right, leading to a faster ECM degradation. Comparing these two experiments already shows the influence of proliferation.
Taking now a look at the right column in figure 32 we see the effects of increased γ to $\gamma = 1.0$. Foremost we see for the tumour cell density a leading edge developing, seperating it into two lumps, with one staying at the center the other invading the tissue and staying where $\nabla(c\nabla e)$ is highest. With increased μ_1 this secession moving into the tissue is getting more pointy, defying differentiability. After $t = 4$ we can observe clear differences regarding ECM and MDE concentration. We see that for higher μ_1 we also get a higher MDE concentration which degrades the ECM visibly faster at the end of the

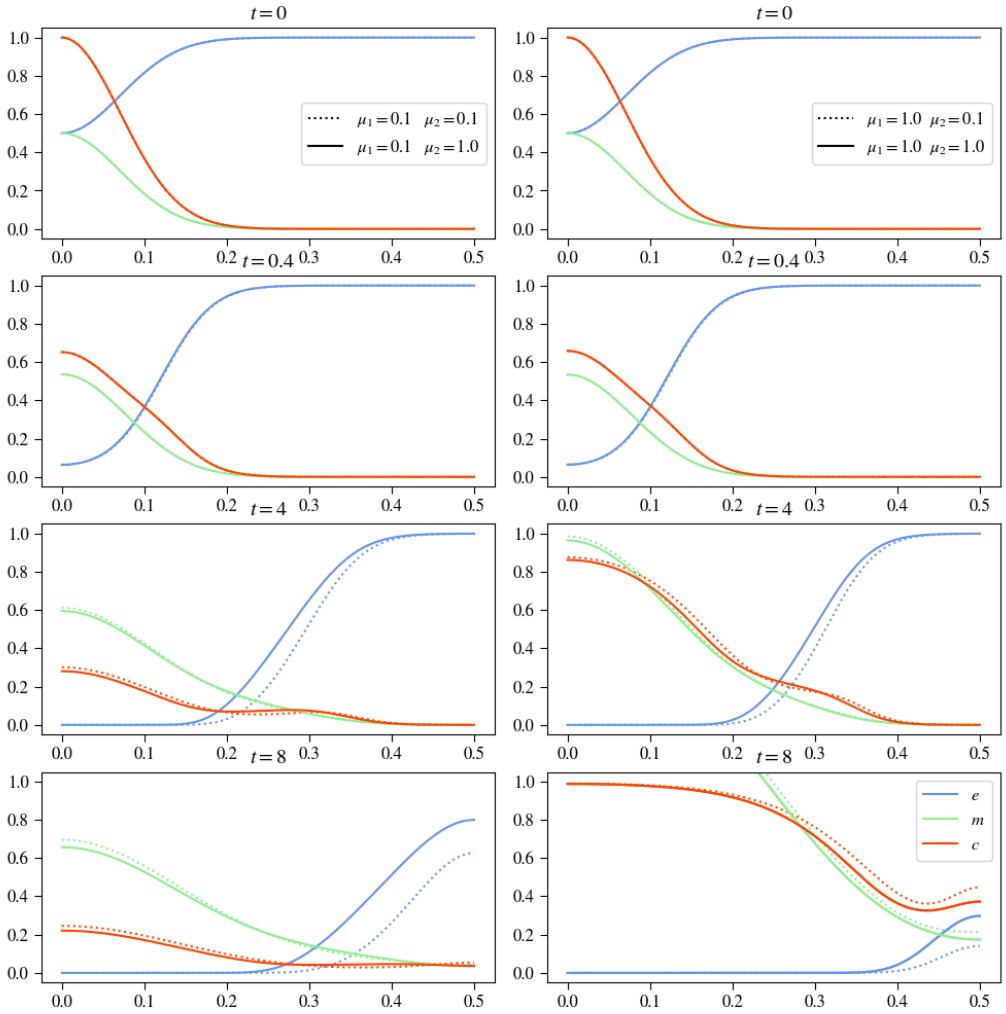

FIGURE 31. Plots show results for varying both μ_1 and μ_2 whilst keeping the other parameters constant.

experiments at $t = 8$. Though interestingly at $t = 4$ the ECM degradataion difference is only minor, at the last point in time the accellerated tumour cell proliferation shows its effet with producignmore MDEs and degrading the ECM considerably faster. What is also interesting to note is that increasing γ and keeping μ_1 low the total area of the MDE concentration is lowered also. Increasing now d_c to 0.1 we see for all experiments in figure 33 that the diffusion of the tumour cells was sufficiently high to evenly distribute the tumour cells constatnly in the space. This constant distribution allows to get an even better look at how μ_1 affects the results, by seeing the lines, describing the tumour cells, rise through time. Looking at the tumour cells over time we can see no observable difference for varying γ. Haptotaxis effects are completely overlaid by diffusion. We see in the left column that if keeping dc high and γ low, but increasing μ_1 leads to higher MDE production rates and also faster ECM degradation. The same behaviour is observable in the right column showing the results for high γ. That we see no difference is clear, since the tumour cell density development is identical over time as mentioned above.

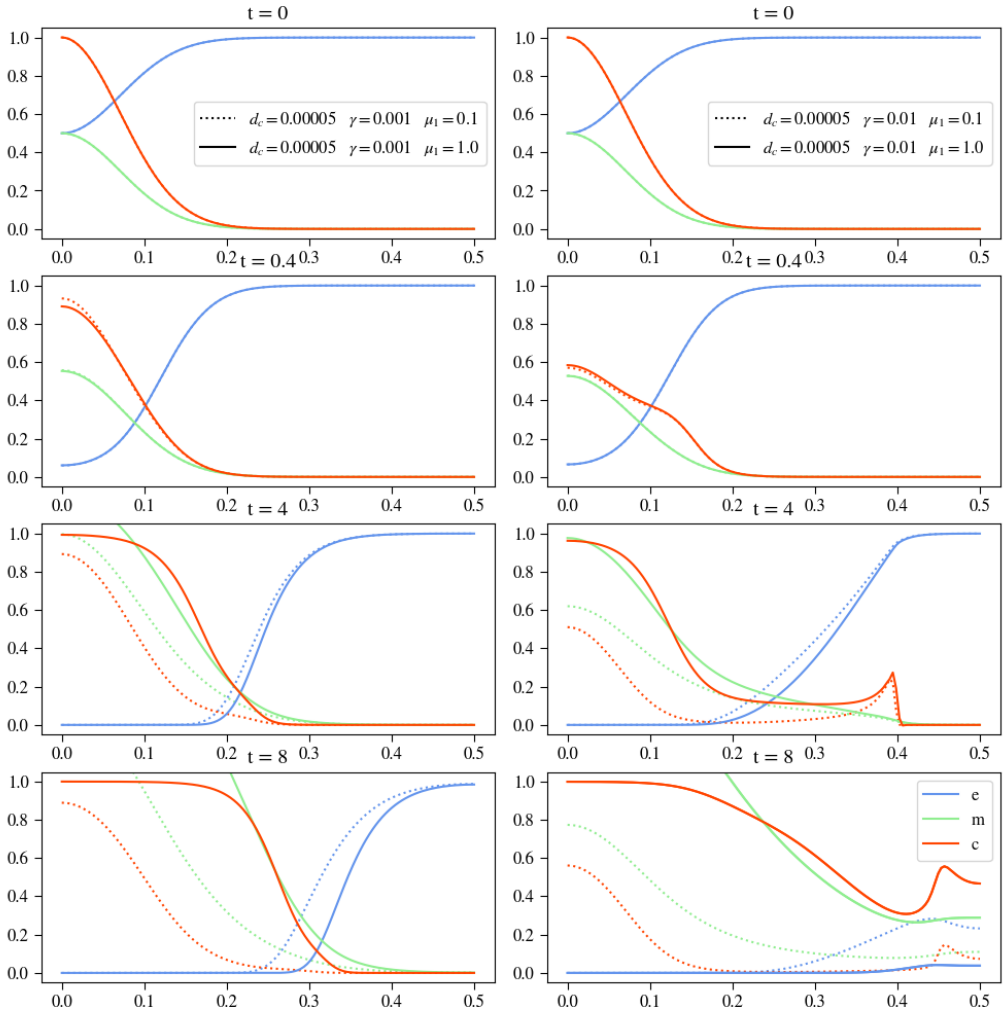

FIGURE 32. Plots show results for varying both d_c, γ and μ_1 whilst keeping the other parameters constant. This plot is the first of two, with the same d_c value for every plot in this figure.

$\eta - \mu_2$ Variation

Varying both η and μ_2 we can expect to see clear changes in the curve describing the ECM concentration. On the left side of figuer 34 we can see the two experiments for low η values and see that increasing μ_1 has only a little effect. Where we could have expected to maybe even see an increase of the ECM we see that the ECM curves for both experiments verify that the renewal factor μ_2 was too low to counter the ECM degradation, even with a low degradation factor. Still between $\mu_2 = 0.1$ and $\mu_2 = 1.0$ there are visibe differences in the degrading speed of the ECM. We can also observe that with the higher renewal term the tumour cell density curve receives more of an effect of haptotaxis resulting in an more streteched curve with only one long lump of tumour cells, where for the lower renewal factor we can still clearly see that there is a secession that invades the tissue and one that stays at the origin. Concerning the MDE curves we can see little difference, for higher μ_2, which meant more stretched tumour cell density, we can also observe a more

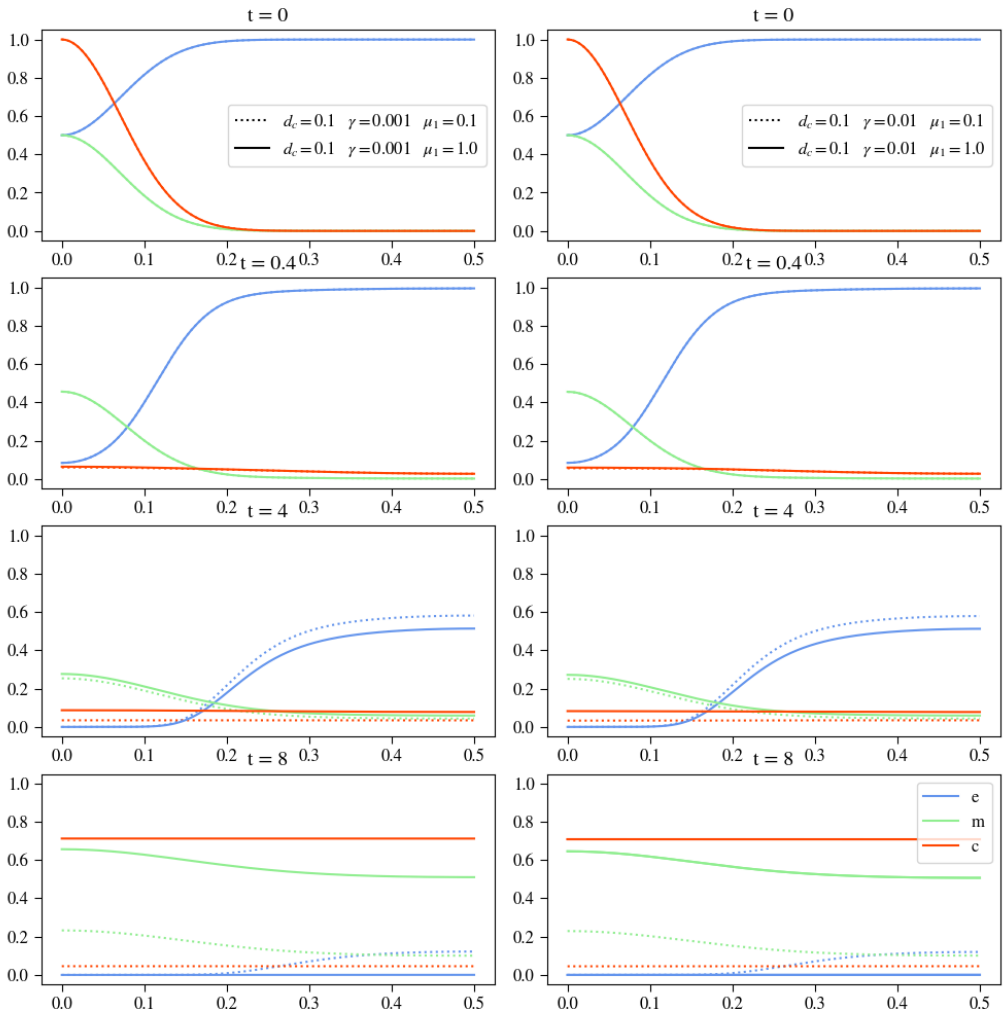

FIGURE 33. Plots show results for varying both d_c, γ and μ_1 whilst keeping the other parameters constant. This plot is the second of two, with the same d_c value for every plot in this figure.

stretched MDE curve with a lower maximum at the origin.
Taking now a look at the experiments with raised η to accellerate the ECM degrading process, we can only see pregnant differences in the curve describing the ECM concentration, the other two look across the steps in time to be widely similar. For the ECM curve we see that the experiment with the lower μ_2 value results in a faster degradation process.

4.3 Three Dimensional Results with Proliferation and Renewal

Lorem ipsum dolor sit amet, consectetuer adipiscing elit. Ut purus elit, vestibulum ut, placerat ac, adipiscing vitae, felis. Curabitur dictum gravida mauris. Nam arcu libero, nonummy eget, consectetuer id, vulputate a, magna. Donec vehicula augue eu neque. Pellentesque habitant morbi tristique senectus et netus et malesuada fames ac turpis

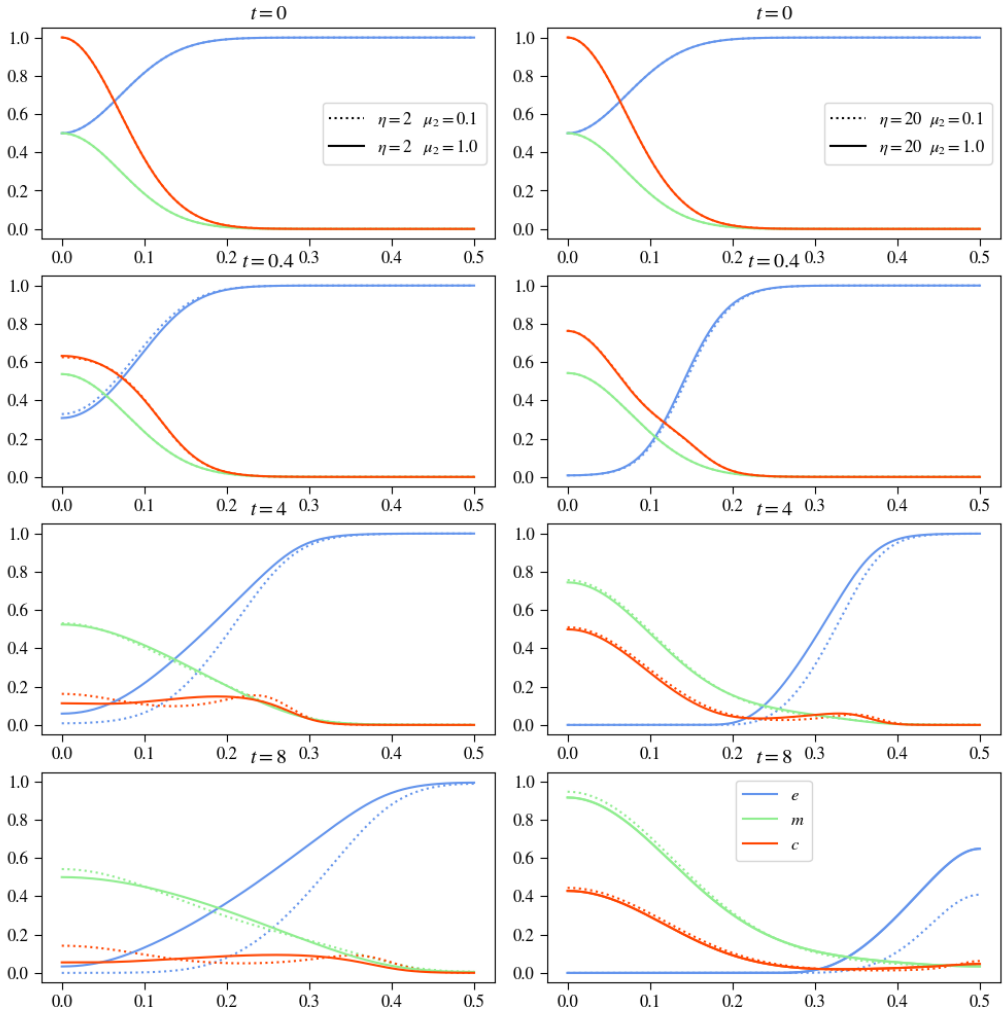

FIGURE 34. Plots show results for varying both η and μ_2 whilst keeping the other parameters constant.

egestas. Mauris ut leo. Cras viverra metus rhoncus sem. Nulla et lectus vestibulum urna fringilla ultrices. Phasellus eu tellus sit amet tortor gravida placerat. Integer sapien est, iaculis in, pretium quis, viverra ac, nunc. Praesent eget sem vel leo ultrices bibendum. Aenean faucibus. Morbi dolor nulla, malesuada eu, pulvinar at, mollis ac, nulla. Curabitur auctor semper nulla. Donec varius orci eget risus. Duis nibh mi, congue eu, accumsan eleifend, sagittis quis, diam. Duis eget orci sit amet orci dignissim rutrum.

Nam dui ligula, fringilla a, euismod sodales, sollicitudin vel, wisi. Morbi auctor lorem non justo. Nam lacus libero, pretium at, lobortis vitae, ultricies et, tellus. Donec aliquet, tortor sed accumsan bibendum, erat ligula aliquet magna, vitae ornare odio metus a mi. Morbi ac orci et nisl hendrerit mollis. Suspendisse ut massa. Cras nec ante. Pellentesque a nulla. Cum sociis natoque penatibus et magnis dis parturient montes, nascetur ridiculus mus. Aliquam tincidunt urna. Nulla ullamcorper vestibulum turpis. Pellentesque cursus luctus mauris.

Nulla malesuada porttitor diam. Donec felis erat, congue non, volutpat at, tincidunt

tristique, libero. Vivamus viverra fermentum felis. Donec nonummy pellentesque ante. Phasellus adipiscing semper elit. Proin fermentum massa ac quam. Sed diam turpis, molestie vitae, placerat a, molestie nec, leo. Maecenas lacinia. Nam ipsum ligula, eleifend at, accumsan nec, suscipit a, ipsum. Morbi blandit ligula feugiat magna. Nunc eleifend consequat lorem. Sed lacinia nulla vitae enim. Pellentesque tincidunt purus vel magna. Integer non enim. Praesent euismod nunc eu purus. Donec bibendum quam in tellus. Nullam cursus pulvinar lectus. Donec et mi. Nam vulputate metus eu enim. Vestibulum pellentesque felis eu massa.

4.4 Heterogenous ECM Structure

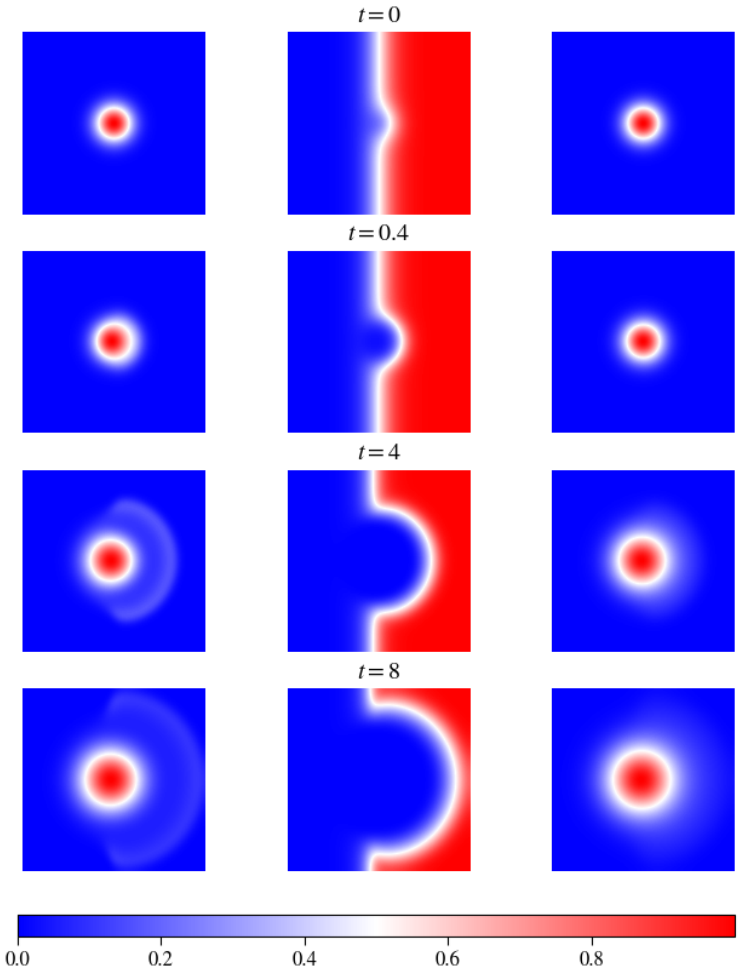

FIGURE 35. 2D Results using a heterogenous ECM with the parameter values: $d_c = 5 \cdot 10^{-4}$, $\gamma = 0.0055$, $\mu_1 = 0.1$, $\eta = 10$, $\mu_2 = 0.5$, $d_m = 1 \cdot 10^{-3}$, $\alpha = 0.3564$, $\beta = 0$; left: tumour cell density, middle: ECM concentration, right: MDE concentration.

Figure 35 you can see the effects using a heterogenous extracellular matrix structure. The plots show in the left column the tumour cell density, the middle column the extracellular matrix concentration and on the right the matrix-degrading enzymes concentration. For the parameters we assumed the basecase studying the model with proliferation.
This experiment describes a more realistic biological scenarino, like seen in figure 1, where the tumour cells are located at the basement membrane of neighboring tissue and have degraded this membrane to invade the surrouding tissue and degrade extracellular matrix there.
In the middle column's first image showing the inital distribution of the experiment you see that the extracellular matrix molecule concentration is only on the right side of the plot, this indicated the neighboring tissue to be invaded. In the center of the same image there is hollow spot where the tumour cells of the initial distribution are located.
After four timesteps you see that the ECM is slowly being degraded and the tumour cells are being pulled by the ECM concentration further into the neighboring tissue. The concentration of the matrix-degrading enzymes shows little differences comparing their behaviour to the experiments done with a homogenous ECM. They only depend indirectly on the ECM, by being produced where the tumour cells are being pulled by the extracellular matrix concentration.
The next point in time shows increased ECM degradation with also further invading tumour cells into the tissue. The tumour cells behave as a semicircular wave moving into the direction of the ECM, you can see the main lump remains at the center, with the edge of having containinig a smaller amount of cells moving outwards. The image describing the matrix-degrading enzyme concentration shows still only minor effects, looking closely we can see that from the center moving to the right there is a slightly higher concentration of them than in the other direction.
The last row depicts the experiment after $t = 8$ timesteps and we see the aforementioned effects propagated. The ECM degradation has continued as well as the invasion of the tumour cells. The wave moving in direction of the remaining extracellular matrix molecules has spread through space and therefore decreased in its strength. The MDEs still show only little influence of the heterogenous ECM with the main lump staying centered and only difficult to recognize more concentration towards the movement of the tumour cells and concentration of the extracellular matrix.
Taking into account different extracellular matrix molecules and structure or physical influences as heat or radiation you can adjust the structure of the ECM and the behaviour of the system to better simulate reallife scenarios of cancer invading tissue.

5 Conclusion and Discussion

Start discussing 2D wihtout proliferation results
Explain how proliferation changes the results
Explain effects of the dimension, going from one dimension to two, going from two to one
Explain ECM strucutre change effects
Lookout on how to extend model chemotaxis/hybrid model, sensitivity analysis

References

1. Anderson, A. Continuous and Discrete Mathematical Models of Tumor-induced Angiogenesis. en. *Bulletin of Mathematical Biology* **60,** 857–899. ISSN: 00928240. http://link.springer.com/10.1006/bulm.1998.0042 (2023) (Sept. 1998).
2. Anderson, A. R. A., Chaplain, M. A. J., Newman, E. L., Steele, R. J. C. & Thompson, A. M. Mathematical Modelling of Tumour Invasion and Metastasis. en. *Journal of Theoretical Medicine* **2,** 129–154. ISSN: 1027-3662, 1607-8578. http://www.hindawi.com/journals/cmmm/2000/490902/abs/ (2023) (2000).
3. Bekisz, S. & Geris, L. Cancer modeling: From mechanistic to data-driven approaches, and from fundamental insights to clinical applications. *Journal of Computational Science* **46.** 20 years of computational science, 101198. ISSN: 1877-7503. https://www.sciencedirect.com/science/article/pii/S1877750320304993 (2020).
4. Hanahan, D. Hallmarks of Cancer: New Dimensions. *Cancer Discovery* **12,** 31–46. ISSN: 2159-8274. eprint: https://aacrjournals.org/cancerdiscovery/article-pdf/12/1/31/3052722/31.pdf. https://doi.org/10.1158/2159-8290.CD-21-1059 (Jan. 2022).
5. Franssen, L. C., Lorenzi, T., Burgess, A. E. F. & Chaplain, M. A. J. A Mathematical Framework for Modelling the Metastatic Spread of Cancer. en. *Bulletin of Mathematical Biology* **81,** 1965–2010. ISSN: 0092-8240, 1522-9602. http://link.springer.com/10.1007/s11538-019-00597-x (2023) (June 2019).
6. Chaplain, M., Lolas, G. & ,The SIMBIOS Centre, Division of Mathematics, University of Dundee, Dundee DD1 4HN. Mathematical modelling of cancer invasion of tissue: dynamic heterogeneity. en. *Networks & Heterogeneous Media* **1,** 399–439. ISSN: 1556-181X. http://aimsciences.org//article/doi/10.3934/nhm.2006.1.399 (2023) (2006).
7. Merino-Casallo, F., Gomez-Benito, M. J., Hervas-Raluy, S. & Garcia-Aznar, J. M. Unravelling cell migration: defining movement from the cell surface. en. *Cell Adh. Migr.* **16,** 25–64 (Dec. 2022).
8. Chaplain, M., McDougall, S. & Anderson, A. MATHEMATIC@ArticleKolev2010, author=Kolev, M. and Zubik-Kowal, B., title=Numerical Solutions for a Model of Tissue Invasion and Migration of Tumour Cells, journal=Computational and Mathematical Methods in Medicine, year=2010, month=Dec, day=30, publisher=Hindawi Publishing Corporation, volume=2011, pages=452320, abstract=The goal of this paper is to construct a new algorithm for the numerical simulations of the evolution of tumour invasion and metastasis. By means of mathematical model equations and their numerical solutions we investigate how cancer cells can produce and secrete matrixdegradative enzymes, degrade extracellular matrix, and invade due to diffusion and haptotactic migration. For the numerical simulationsof the interactions between the tumour cells and the surrounding tissue, we apply numerical approximations, which are spectrally accurateand based on small amounts of grid-points. Our numerical experiments illustrate the metastatic ability of tu-

mour cells.,@article10.14492/hokmj/1520928060, author = Akio ITO, title = Large-time behavior of solutions to a tumor invasion model of Chaplain–Anderson type with quasi-variational structure, volume = 47, journal = Hokkaido Mathematical Journal, number = 1, publisher = Hokkaido University, Department of Mathematics, pages = 33 – 67, keywords = large-time behavior, quasi-variational structure, tumor invasion, year = 2018, doi = 10.14492/hokmj/1520928060, URL = https://doi.org/10.14492/hokmj/1520928060 doi=10.1155/2011/452320, url=https://doi.org/10.115
AL MODELING OF TUMOR-INDUCED ANGIOGENESIS. en. *Annual Review of Biomedical Engineering* **8,** 233–257. ISSN: 1523-9829, 1545-4274. https://www.annualreviews.org/doi/10.1146/annurev.bioeng.8.061505.095807 (2023) (Aug. 2006).

9. Kitware, Inc. *ParaView* https://www.paraview.org/. Zuletzt abgerufen am [Datum]. 2022.

10. Stéphanou, A., McDougall, S., Anderson, A. & Chaplain, M. Mathematical modelling of the influence of blood rheological properties upon adaptative tumour-induced angiogenesis. *Mathematical and Computer Modelling* **44.** Advances in Business Modeling and Decision Technologies [pp. 1-95], 96–123. ISSN: 0895-7177. https://www.sciencedirect.com/science/article/pii/S0895717705004565 (2006).

11. Kolev, M. & Zubik-Kowal, B. Numerical Solutions for a Model of Tissue Invasion and Migration of Tumour Cells. *Computational and Mathematical Methods in Medicine* **2011,** 452320. ISSN: 1748-670X. https://doi.org/10.1155/2011/452320 (Dec. 2010).